Simultaneous assessment of the $YBa_2Cu_3O_{6+z}$ thermodynamics under the linear error model

E.B. Rudnyi, V.V. Kuzmenko, and G.F. Voronin

Chemistry Department, Moscow State University, 119899 Moscow, Russia

About 3000 experimental points obtained in 220 miscellaneous experiments published in 57 papers have been processed simultaneously in order to obtain the most reliable Gibbs energy of the $YBa_2Cu_3O_{6+z}$ phase in the temperature range from 250 K to 1300 K. All other thermodynamics properties of the phase including the conditions for the tetragonal-orthorhombic phase transition and the miscibility gap at lower temperatures are derived from the assessed Gibbs energy. The linear error model introduced recently by one of authors has been employed for the simultaneous assessment. The results obtained are compared with those of the conventional weight least squares method and the benefit of the new approach is discussed. Another problem in simultaneous assessment that is also considered is visualizing the quality of the fit. New types of graphs (partly based on the linear error model) that facilitate visualizing the quality of the fit are presented.

Key words: high-temperature superconductor, chemical thermodynamics, Gibbs energy, enthalpy of formation, entropy, heat capacity, lattice model, visualizing quality of the fit, maximum likelihood, mixed model, variance component.

Contents

List of Tables

List of Figures

1.   Introduction

The $YBa_2Cu_3O_{6+z}$ phase is the first high temperature superconductor that has been found to exist above the liquid nitrogen temperature. Its properties have been studied in many laboratories and numerous experimental values are currently available. The goal of the present study is to compile all the experimental values related to the thermodynamic properties of the $YBa_2Cu_3O_{6+z}$ phase and to assess the most reliable Gibbs energy as a function of temperature and non-stoichiometry index z. When the Gibbs energy of the phase is known all the other thermodynamic properties can be obtained by means of the thermodynamic laws.

The present work is the continuation of 93DEG/VOR (see also 90DEG, 90DEG2, 90MER/DEG, 91VOR/DEG) where the thermodynamic model of the $YBa_2Cu_3O_{6+z}$ phase has been suggested and the Gibbs energy has been already estimated. In the present work,

the new experimental results that have appeared recently have been included in the assessment, and the more attention has been paid to the statistical treatment.

We are aware of other papers that have been devoted to the assessment of the $YBa_2Cu_3O_{6+z}$ phase thermodynamics since 1991 (discussion of the previous attempts can be found in 91VOR/DEG). However, in our view, none of them has reached the final goal.

The $YBa_2Cu_3O_{6+z}$ thermodynamic model in 91LEE/LEE treats this compound as a single phase and hence the results of 91LEE/LEE do not allow us to distinguish between the $YBa_2Cu_3O_{6+z}$ orthorhombic and tetragonal modifications. This is very unfortunate because only the orthorhombic phase possesses superconducting properties, and thus all the practitioners would like to know what a modification will be formed under given conditions.

93PLE/ALT have assessed the thermodynamic properties of the $YBa_2Cu_3O_{6+z}$ phase by means of a step-by-step approach. This means that they evaluated the heat capacity, the enthalpy, oxygen partial pressure and other properties consecutively without employing any uniform model. As a result, the equations given do not obey the thermodynamic laws. For example, Eq. (12) in this paper contradicts with Eqs (9) and (11), *i.e.*, according to the thermodynamic laws these equations can not be held simultaneously.

Recently 96BOU/HAC have published a paper where they have claimed that an assessment of $YBa_2Cu_3O_{6+z}$ phase thermodynamics has been accomplished (none of Degterov and Voronin's works have been cited). Unfortunately, all that is available there is a sentence "we did it". In order to discuss this statement we have to wait until some more details are published.

For a given system, the more experiments that are conducted, the more reliable the results. Nobody seems to argue with this statement. On the other hand, however, the results of the distinct experiments usually differ more between each other that the reproducibility error in a single experiment. In this respect, the $YBa_2Cu_3O_{6+z}$ phase is a very good example because we do have a lot of data that have been published since it has been discovered: more than 3000 experimental points obtained in about 220 experiments conducted by nearly 50 laboratories. Nevertheless, as one may expect, the scatter of the results is rather huge and mere processing of all the results makes no sense at all.

The quality of different experiments is certainly different, and moreover, the quality of the result presentation is also different. For example, many authors have presented their experimental results as figures only. With advent of the digital scanners it is relatively easy to convert these figures to numbers but the question how these figures have been made remains unanswered.

Traditionally the question of the data quality has been solved by means of the weight least squares when an expert assigned a weight to each experimental point a priori based on her preferences. The main problem on this way is the subjectivity. It is relatively easy to say that the weight for this point should be equal to one and for that point is equal to one and half. It is not that easy though to explain how you have come to that conclusion. It should be especially mentioned that we are not against subjectivity. Whether we want it or not, the subjectivity can never be completely excluded in practical applications. Hope for

the "golden" algorithm that would just take raw data and produce the true answer is ungrounded because before data processing we must always postulate some hypothesis than can not be proved empirically in that treatment.

Still, the subjectivity can be put under stronger control than in the case of the weight least squares as has been shown by 96RUD, 97RUD and 97KUZ/USP. The new advanced methods of mathematical statistics allow the expert to make the qualitative conclusions only and let the formal methods do the rest. Making qualitative statements is much easier for the human being, and furthermore, this also leads us to the formal way of expressing the qualitative conclusions that are necessary for the simultaneous assessment.

Thus, the goal of the present work is twofold: first, to obtain the most reliable Gibbs energy of the $YBa_2Cu_3O_{6+z}$ phase, second, to discuss with this example the new approaches for the simultaneous assessment. We will start with the description of the thermodynamic model of the phase in Section 2 and available experimental results in Section 3. Then in Section 4, we will review the linear error model (see 96RUD and 97RUD for details) and describe its application to the thermodynamics of the $YBa_2Cu_3O_{6+z}$ phase. Section 5 is devoted to another important question in the simultaneous assessment: the visual comparison of different solutions. In Section 6, the results obtained are compared with those in the weight least squares. Finally, Section 7 summarizes the methodological results that, in our view, have been achieved in the present study.

2.   Thermodynamic model

The thermodynamic model of the $YBa_2Cu_3O_{6+z}$ phase has been developed earlier by Voronin and Degterov in 90DEG, 90DEG2, 90MER/DEG, 91VOR/DEG and 93DEG/VOR. Below there is just a brief review and 92VOR/DEG should be consulted for the complete description of the model.

The $YBa_2Cu_3O_{6+z}$ phase has a layered structure $(CuO_z)(BaO)(CuO_2)(Y)(CuO_2)(BaO)$ of the perovskite type. Only one of the three copper-based layers, so called basal plane, is responsible for the oxygen non-stoichiometry (adsorption, desorption and ordering). All other layers are considered to be stoichiometric and the overall formula unit can be written as

$$[Y^{+3}(Ba^{+2})_2(Cu^{+2})_2(O^{-2})_6] (Cu^{+1}, Cu^{+3})_1^{(m)}(O^{-2}, Va)_1^{(a)}(O^{-2}, Va)_1^{(b)} \qquad (1)$$
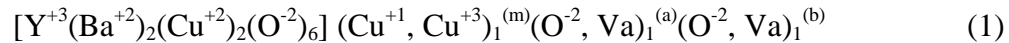
Here the basal plane is considered to comprise three sublattices: a cation sublattice for copper and two anion sublattices filled with the atoms of oxygen and vacancies (Va). It was necessary to introduce the two oxygen sublattices because the $YBa_2Cu_3O_{6+z}$ phase was found to exist in two modifications, tetragonal and orthorhombic. The occupancies of the sublattices (a) and (b) are the same in the tetragonal form, and the sublattice (b) is richer by oxygen in the orthorhombic form.

The sublattice model leads to the expression for the phase Gibbs energy as follows (complete calculus are in 91VOR/DEG):

$$\Delta_{ox}G(T, z, x) = g_1(T) + g_2(T)z + z(1 - z)\Sigma_i a_i(T)(1 - z)^i + (c^2 - x^2)\Sigma_i b_i(T)(1 - z)^{i-1}$$
$$+ T[(c + x) \ln (c + x) + (c - x) \ln (c - x) + (1 - c + x) \ln (1 - c + x)$$
$$+ (1 - c - x) \ln (1 - c - x) + z \ln z + (1 - z) \ln (1 - z)] \qquad (2)$$

where z is the shoichiometry index of the basal plane ($0 \leq z \leq 1$), c is short for $z/2$, x is the order parameter ($0 \leq x \leq z/2$), $g_i(T)$, $a_i(T)$ and $b_i(T)$ are some temperature functions to be determined. $\Delta_{ox}G$ stands for the Gibbs energy of formation from the oxides, Y_2O_3, BaO, CuO, and oxygen $i.e.,$ the Gibbs energy of reaction

$$0.5Y_2O_3 + 2BaO + 3CuO + (0.5z\text{-}0.25)O_2 = YBa_2Cu_3O_{6+z} \qquad (3)$$
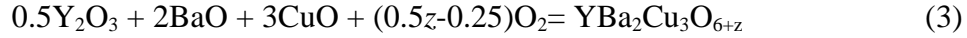
The thermodynamic properties of the oxides and oxygen employed in the present work are listed in Table 1.

The order parameter x is defined as the difference between the oxygen occupancies y_O in the sublattices (b) and (a) as follows

$$x = (y_O^{(b)} - y_O^{(a)})/2 = z/2 - y_O^{(a)} \qquad (4)$$

Thus, x should be equal to zero for the tetragonal phase and it is inside the interval $0 < x < z/2$ for the orthorhombic phase. The parameter x is considered as "inner", that is for all the thermodynamic functions at equilibrium we have just two independent variables, the temperature T and the index z. The value of x at any given T and z can be determined by minimizing Eq. (2) over x, or by equating to zero the partial derivative of $\Delta_{ox}G$ in respect to x

$$(\partial\Delta_{ox}G/\partial x)_{T,z} = 0 \qquad (5)$$

This equation can not be solved in the closed form but this is quite an easy task for the modern numerical analysis. The only precaution that should be taken here is to choose the right root of Eq. (5) that corresponds to the minimum of Eq. (2).

The "inner" variable x makes the model a bit unusual even though this is quite an ordinary approach for the modern solution models. Eq. (2) describes function $\Delta_{ox}G(T, z, x)$ in three variables in the closed form. In practice, function $\Delta_{ox}G(T, z)$ is required because in the case of $YBa_2Cu_3O_{6+z}$ it is possible to control two external variables only. Then, the order parameter x is assumed to reach the equilibrium value x_{eq} and we have

$$\Delta_{ox}G(T, z) = \Delta_{ox}G\{T, z, x_{eq}(T, z)\} \qquad (6)$$

where function $x_{eq}(T, z)$ represents the solution of Eq. (5). Because the latter is not available in the closed form, Eq. (6) can be considered as an algorithm that suggests computing $\Delta_{ox}G(T, z)$ in two steps: first solving Eq. (5) numerically for the equilibrium value of x and then substituting it in Eq. (2). It is worthy noting that the same is held for other thermodynamic properties of the $YBa_2Cu_3O_{6+z}$ phase, for example $\Delta_{ox}H(T, z) = \Delta_{ox}H\{T, z, x_{eq}(T, z)\}$. The use of numerical methods changes nothing in principle, we can safely think that function $x_{eq}(T, z)$ is completely known, and the only difference is that calculations become unworkable without computers.

Let us stress once more that the lattice model that brought Eq. (2) forth gives the uniform description for both modifications of the $YBa_2Cu_3O_{6+z}$ phase. Provided all the parameters in Eq. (2) are known the type of the phase at any given T and z is determined

by function $x_{eq}(T, z)$ that is doubtlessly defined by Eq. (2) itself. If the equilibrium value of x is equal to zero then we have the tetragonal phase, otherwise the orthorhombic phase is more stable. The phase border between the two modifications (the transition temperature at the given index z) can be found by solving the next equation

$$(\partial^2 \Delta_{ox} G / \partial x^2)_{T,z}|_{x=0} = 0 \tag{7}$$

Again, in the general case this can be done by numerical methods only.

While writing Eq. (2) down we have neglected the influence of the hydrostatic pressure, *i.e.*, the term $\int_{p^o}^{p} V_m \, \mathrm{d}\, p$ because it is usually small for condensed phases. In the last expression p^o is the standard pressure for which the Eq. (2) is supposed to be held (in the present work $p^o = 101325$ Pa). However, in our model the Gibbs energy of the $YBa_2Cu_3O_{6+z}$ phase depends heavily on the partial pressure of oxygen in the surrounding atmosphere. If there is the gas phase in equilibrium with $YBa_2Cu_3O_{6+z}$ then according to the equilibrium criterion the oxygen partial pressure there must be equal to

$$\ln \{p(O_2)/p^o\} = 2\Delta_{ox} G'_O / RT \tag{8}$$

where $\Delta_{ox} G'_O$ is the partial Gibbs energy, *i.e.*, the partial derivatives

$$\Delta_{ox} G'_O \equiv \{\partial \Delta_{ox} G(T, z)/\partial z\}_T \tag{9}$$

Taking into account Eq. (6) and the differentiation rule for a compound function we obtain

$$\Delta_{ox} G'_O = \{\partial \Delta_{ox} G(T, z, x)/\partial z\}_{T,x} + \{\partial \Delta_{ox} G(T, z, x)/\partial x\}_{T,z} \{\partial x_{eq}(T, z)/\partial z\}_T \tag{10}$$

The second term vanishes because of Eq. (5) and finally the partial Gibbs energy takes the next form

$$\Delta_{ox} G'_O = \{\partial \Delta_{ox} G(T, z, x)/\partial z\}_{T,x} \tag{11}$$

In many experiments it was the oxygen partial pressure that was fixed externally and then the index z should be considered as a function, $z\{p(O_2), T\}$. The latter is implicitly given by Eqs (5), (8) and (11), which should be solved for z at given oxygen partial pressure and temperature. Then, all the thermodynamic properties are also can be estimated under such conditions. For example, the Gibbs energy can be computed as follows

$$\Delta_{ox} G\{p(O_2), T\} = \Delta_{ox} G\{T, z[p(O_2), T], x_{eq}(T, z[p(O_2), T])\} \tag{12}$$

Certainly, we should rely again on numerical methods here.

The $YBa_2Cu_3O_{6+z}$ phase can be considered as a two-component solution and the formation of the miscibility gap can not be excluded. Actually there are evidences that that the miscibility gap with the upper critical temperature should occur in the $YBa_2Cu_3O_{6+z}$ phase about room temperatures. The criterion for the complete miscibility requires Eq. (2) as a function of z at constant temperature to be convex, or the partial Gibbs energy $\Delta_{ox} G'_O$ (and then the oxygen partial pressure) to monotonously increase with the growth of z. If at

some temperature this is not the case, then we have a miscibility gap and its borders can be found by solving a system of the two equations for two unknowns, z' and z'' ($z' \neq z''$)

$$\Delta_{ox}G(T, z'') - \Delta_{ox}G(T, z') = \Delta_{ox}G'_O(T, z')(z'' - z') = \Delta_{ox}G'_O(T, z'')(z'' - z') \qquad (13)$$

All other thermodynamic properties of the $YBa_2Cu_3O_{6+z}$ phase can also be found provided the Gibbs energy (Eq. 2) is known. Taking into account that $H = -T^2\{\partial(G/T)/\partial T\}_p$ and $S = -\{\partial G/\partial T\}_p$ and then following the same way as for the partial Gibbs energy (see Eqs 9 to 11) we have

$$\Delta_{ox}H = -T^2\{[\partial\Delta_{ox}G(T, z, x)/T]/\partial T\}_{z,x} \qquad (14)$$

$$\Delta_{ox}S = -\{\partial\Delta_{ox}G(T, z, x)/\partial T\}_{z,x} \qquad (15)$$

Then, the thermodynamic relationship $C_p = (\partial H/\partial T)_p$ lead us to the computational expression for the heat capacity as follows

$$\Delta_{ox}C_{pz} = \{\partial\Delta_{ox}H(T, z, x)/\partial T\}_{z,x} + \{\partial\Delta_{ox}H(T, z, x)/\partial x\}_{T,z}\{\partial x_{eq}(T, z)/\partial T\}_z \qquad (16)$$

Note that the second term is not equal to zero here and that in the case of $YBa_2Cu_3O_{6+z}$ some other heat capacities can be also introduced (see 93DEG/VOR). Eqs (15) and (16) give the entropy and the heat capacity of reaction (3). The absolute values can be also obtained as follows

$$S = \Delta_{ox}S + 0.5S_{Y2O3} + 2S_{BaO} + 3S_{CuO} + (z/2 - 0.25)S_{O2} \qquad (17)$$

$$C_{pz} = \Delta_{ox}C_{pz} + 0.5C_{p,Y2O3} + 2C_{p,BaO} + 3C_{p,CuO} + (z/2 - 0.25)C_{p,O2} \qquad (18)$$

Another thermodynamic property that has been measured for the $YBa_2Cu_3O_{6+z}$ phase is the partial enthalpy. After analogous considerations as above it can be computed as follows

$$\Delta_{ox}H'_O = \{\partial\Delta_{ox}H(T, z)/\partial z\}_T = \{\partial\Delta_{ox}H(T, z, x)/\partial z\}_{T,x}$$
$$+ \{\partial\Delta_{ox}H(T, z, x)/\partial x\}_{T,z}\{\partial x_{eq}(T, z)/\partial z\}_T \qquad (19)$$

Therefore, if the values of all the parameters in Eq. (2) are known then each thermodynamic property of the $YBa_2Cu_3O_{6+z}$ phase is also known, and then the assessment of the $YBa_2Cu_3O_{6+z}$ thermodynamics is equivalent to determining the unknown temperature functions, $g_i(T)$, $a(T)_i$, $b_i(T)$ in Eq. (2). The latter is possible if we choose some analytical function in temperature and put unknown parameters within it. Along this way, the traditional approach for solution thermodynamics was followed when the temperature function is based on the expression for the Gibbs energy of the stoichiometric compounds that in turn depends on the temperature dependence of the heat capacity. However, the form of the heat capacity function accepted in the present work

$$C_p = k_0 + k_1T^{-0.5} + k_2T^{-2} + k_3T^{-3} \qquad (20)$$

does not enjoy widespread use yet. Eq. (20) is invented by 85BER/BRO who have demonstrated its advantage as compared with traditional Maier and Kelley's and other equations. Provided k_1 and k_2 are negative, Eq. (20) ensures that heat capacity approaches the high temperature limit predicted by lattice vibrational theory and thus this makes extrapolating the low-temperatures heat capacities to high temperatures rather reliable. According to 85BER/BRO, Eq. (20) can be safely used from 250 K to 3000 K and this

has set the lower limit for the temperature interval in the present work. Eq. (20) leads to the temperature dependence of the Gibbs energy as follows

$$G - H_{298} = A + B\,T + C\,T\ln T + D\,T^{0.5} + E\,T^{-1} + F\,T^{-2} \tag{21}$$

where two additional parameters have appeared during two integrations.

3.   Literature experimental values

In this section the experiments are classified according to the measured properties of the $YBa_2Cu_3O_{6+z}$ phase. For each group of experiments a measured property and variables under control are considered first. As we neglected the hydrostatic pressure, the $YBa_2Cu_3O_{6+z}$ phase has two degrees of freedom and thus two variables should be controlled in any experiment. The only exception is experiment for determining the line of the phase transition when according to the Gibbs rule the $YBa_2Cu_3O_{6+z}$ phase has one degree of freedom. A typical notation for the experimental point is

$$\{y_{ij},\ u_{ij},\ v_i\} \tag{22}$$

where the index i enumerates the experiments, j does the experimental points inside the i-th experiment ($j = 1, ..., N_i$), y_{ij} is what has been measured, u_{ij} is what has been changed and v_i is what has been fixed during this experiment.

Then the relationship between the measured property and the controlled variables is discussed. In the general form it can be expressed as

$$y_{ij} = y_{ij}^{calc}\{u_{ij},\ v_i;\ \Theta\} + \varepsilon_{ij} \tag{23}$$

where y_{ij}^{calc} is the value that is calculated by thermodynamic laws at given u_{ij} and v_i and that differs from the experimentally measured y_{ij} by the experimental error ε_{ij}. The discussion of errors will be delayed until Section 4. Θ is the vector of unknown parameters to be determined. As was discussed in the previous section, all the thermodynamics properties of the $YBa_2Cu_3O_{6+z}$ phase, y_{ij}^{calc} can be obtained from Eq. (2) by means some algebraic and/or numerical methods. This means that vector Θ contains the same set of unknown parameters for all the equations described below. Note that some parameters may vanish during differentiation of Eq. (2).

The results of the experiments in each category is possible to compare between each other directly. The results of this comparison and the quality of experiments are discussed and the further partition of the experiments in each group into smaller sets of about the same quality is presented. The comparison between different experimental groups is impossible without simultaneous assessment and will be discussed in Sections 4 and 5.

Figures with the experimental points are given for most experiments. On the figures there are three solutions also: two of them are obtained in the present work (ML and WLS) and one is taken from the previous assessment by 93DEG/VOR. The solutions are discussed later in Sections 4 to 6.

Table 2 summarizes all the experimental information available. It contains the codes assigned to the experiments, references, and information on experiments: the number of experimental points, whether the experiment is included in the assessment (column *inc*)

and the value of v_i. The different experimental groups are separated by solid lines and subgroups of about the same quality are by dashed lines. The division into the experimental groups is summed up in Table 3.

3.1. Tetragonal-orthorhombic phase transition and oxygen occupancies

It seems that first measurements related to thermodynamic properties of the $YBa_2Cu_3O_{6+z}$ phase were the determination of temperatures of the tetragonal-orthorhombic phase transition. In a typical experiment the sample of the $YBa_2Cu_3O_{6+z}$ phase was heated or cooled in the controlled atmosphere with the known oxygen partial pressure. The phase transition was detected by the bend at the TGA or resistivity curve or by X-ray method. Then we have a number of experimental points $\{T_{ij}, \ln p(O_2)_{ij}\}$ (see Fig. 1 and Table 2). One can compute the temperature of the phase transition T_{ij}^{calc} at a given oxygen partial pressure by solving the system of the two equations (7) and (8) for the two unknowns z and T assuming that x is equal to zero.

The experiments carried out by 88MEU/RUP and 89MEU/RUP were quite similar except that the oxygen partial pressure was not fixed during the heating/cooling cycle. The problem is that the authors have presented not the original experimental values in the form $\{T_{ij}, \ln p(O_2)_{ij}\}$ but rather recalculated $p(O_2)_{ij}$ to the index z_{ij} according to their own measurements. Thus, here we have the experimental points in the form $\{T_{ij}, z_{ij}\}$ (Table 2 and Fig. 2). The calculation of T_{ij}^{calc} at the given z_{ij} is easier than in the previous case. It is necessary to solve one equation (7) for one unknown T. In the simplest case it is even possible in the closed form. However, it should be especially mentioned that in this case we don't have the results of the original experiments, and it is very difficult to estimate uncertainties in the values of z_{ij} ascribed by the authors to the measured values of the temperature of the phase transition.

The oxygen occupancies in the sublattices (a) and (b) (see Eq. 1) have been measured by 87JOR/BEN and 88IKE/NAG and according to Eq. (4) this gives us the equilibrium value of the order parameter x. The neutron diffraction has been employed in the first work and the profile fitting of X-ray diffraction reflections in the second one. The experiments were carried out at the constant oxygen partial pressure at several temperatures and the experimental points look like $\{x_{ij}, T_{ij}, \ln p(O_2)_i\}$ (see Table 2 and Fig. 3). Computing the value of x_{ij}^{calc} at given temperature and oxygen partial pressure is to be done numerically by solving the system of Eqs (5) and (8) for two unknowns, index z and the value of the equilibrium order parameter x.

3.2. Oxygen partial properties

In most experiments, the relationship between the oxygen partial pressure over the $YBa_2Cu_3O_{6+z}$ phase, index z and temperature has been studied. Because of the Gibbs phase rule one can state that $f\{\ln p(O_2), T, z\} = 0$. There are many possibilities to study this two-dimensional surface and it seems that all of them have been implemented in the case of the $YBa_2Cu_3O_{6+z}$ phase.

It is rather simple to control the oxygen partial pressure over the $YBa_2Cu_3O_{6+z}$ phase. Then the thermogravimetry (TGA) allows us to measure the weight of the sample as a function of temperature and thus to measure the dependence of index z from temperature at constant partial pressure. This gives the experimental points in the form $\{z_{ij}, T_{ij}, \ln p(O_2)_i\}$ and it is possible to calculate z_{ij}^{calc} by solving the system of Eqs (5) and (8) for the two unknowns, index z and the value of the equilibrium order parameter x.

All the experiments in this category were divided into three groups Z_b, Z_g, and Z (see Table 3) based on the fact that most researchers have presented the results in the graphic form. The results in group Z are available as numbers and they should be considered as most reliable. It is interesting, that if alternatively we divided the papers based on our expert opinion, neglecting whether there are numeric results or not, the same works that are now in group Z have been marked as the best ones. For the rest of the papers numerical values have been obtained from figures by means of scanning and they were put into two groups as follows. The results in group Z_g are in reasonable agreement with group Z and the results in group Z_b are not.

Fig. 4 and Fig. 5 display the results of group Z (89LIN/HUN, 89VER/BRU and 92CON/KAR).

Another opportunity is to study isotherms, that is the dependence of $\ln p(O_2)$ from z at constant temperature. This gives experimental points in the form of $\{\ln p(O_2)_{ij}, z_{ij}, T_i\}$. The techniques employed here were the emf method, volumetric apparatus and TGA (see Table 2). The work of 89MEU/NAE is also included in this group even though the real experimental path differed from the isotherm. The reason is that the results are available in this form only. It happens that computing $p(O_2)_{ij}^{calc}$ at given index z and temperature is simpler than in the previous case. Here the system of the two equations, (5) and (8) can be simplified. First, Eq. (5) is to be solved numerically and then it is possible to utilize Eq. (8) directly in the closed form.

As for the previos category, most results are available in the graphic form and the experiments were partitioned into three groups, O, O_g, and O_b by means of analogous considerations. Only authors of the three works, 89GER/PIC, 91SCH/HAR and 92MAT/JAC have given the numerical values (group O) and their results are shown in Fig. 6 and in Fig. 7.

89VER/BRU have made the special apparatus based on the volumetric approach to maintain the constant value of index z while heating or cooling the $YBa_2Cu_3O_{6+z}$. As a result, they have managed to obtain the results in the form of $\{\ln p(O_2)_{ij}, T_{ij}, z_i\}$. The computation of the $p(O_2)_{ij}^{calc}$ here is analogous to that in the case of the isotherms. The results are shown in Fig. 8.

A different experimental path has been implemented by 94TAR/GUS during the traditional volumetric experiment. The total pressure was measured as a function of temperature at constant total volume and after assumption that the gas phase contains molecular oxygen only the experimental points look like $\{\ln p(O_2)_{ij}, T_{ij}, V_i, z_i^o, m_i^o\}$, where V_i is the volume of the chamber, z_i^o is the index and m_i^o is the mass of the original sample. During the experiment index z has changed because some oxygen escaped from $YBa_2Cu_3O_{6+z}$ to the gas phase. Assuming that molecular oxygen obeys the perfect gas law

and neglecting the volume of the condensed phase the current index z_{ij} can be estimated as follows

$$z_{ij} = z_i^o - 2p(O_2)_{ij}^{calc} V_i \{M(YBa_2Cu_3O_6) + M(O_2)z_i^o\}/(RT_{ij}m_i^o) \qquad (24)$$

Computing $p(O_2)_{ij}^{calc}(T_{ij}, V_i, m_i^o, z_i^o)$ is a bit more difficult. To this end, one has to solve a system of three equations, (5), (8) and (24) for three unknowns, $\ln p(O_2)_{ij}^{calc}$, index z and the equilibrium order parameter x. The results will be discussed in Section 5.

Oxygen partial enthalpies (see Eq. 19) have been measured by reaction microcalorimetry in 89GER/PIC as a function of index z at 873 K, *i.e.*, we have experimental points in the form of $\{\Delta_{ox}H'_{O,ij}, z_{ij}, T_i\}$. Computing $\Delta_{ox}H'_{O,ij}{}^{calc}$ is rather straightforward. The results are in Fig. 9.

89PAR/NAV have also employed high temperature reaction calorimetry, however the experiment was carried out differently and the results here are available as transposed-temperatures-drop enthalpies

$$YBa_2Cu_3O_{6+z'}(T') = YBa_2Cu_3O_{6+z''}(T'') + (z'/2 - z''/2)O_2(T'') \qquad (25)$$

It is possible to convert the measured enthalpies to the oxygen partial enthalpies but we have preferred to employ them directly in the form of $\{\Delta H_{ij}, z'_{ij}, T'_i, z''_i, T''_i\}$ (see Fig. 10). The use of direct experimental values may look as more difficult procedure but this excludes a lot of ambiguity otherwise introduced during the conversion of the primary experimental results. Enthalpy of Reaction (25), $\Delta H_{ij}{}^{calc}(z'_{ij}, T'_i, z''_i, T''_i)$ can be easily calculated from the enthalpies of $YBa_2Cu_3O_{6+z}$ phase and oxides as follows

$$\Delta H_{ij}{}^{calc} = \Delta_{ox}H(T''_i, z''_i) - \Delta_{ox}H(T_i, z'_{ij}) + 0.5\{H(T''_i) - H(T'_i)\}_{Y2O3}$$
$$+ 2\{H(T''_i) - H(T'_i)\}_{BaO} + 3\{H(T''_i) - H(T'_i)\}_{CuO} + (z'/2 - 0.25)\{H(T''_i) - H(T'_i)\}_{O2} \quad (26)$$

3.3. *Integral properties*

Thermodynamics properties discussed so far would be enough to predict the behavior of the $YBa_2Cu_3O_{6+z}$ phase by itself even though they do not allow us to estimate temperature function $g_1(T)$ in Eq. (2) because it disappears during the differentiation in respect to index z. Yet, in order to predict results of the interaction with other substances one has got to know the Gibbs energy as a whole. To this end, we have experiments available when the integral Gibbs energy, the enthalpy, the entropy and the heat capacity have been measured.

Oxygen adsorption and desorption from the $YBa_2Cu_3O_{6+z}$ phase below $\approx$ 450 K can be considered as "frozen" and index z at these temperatures is not controlled by the external oxygen partial pressure anymore. This allows us to measure the heat capacity, C_{pz} as a function of temperature at constant z. The experimental point has a form of $\{C_{pz,ij}, T_{ij}, z_i\}$ and the corresponding value of $C_{pz,ij}{}^{calc}(T_{ij}, z_i)$ can be estimated by Eqs (16) and (18). All the available values are divided into the two groups: low-temperature heat capacity measured by adiabatic calorimetry (see Fig. 12, Table 2, and Table 3) and high temperature heat capacity measured by differential scanning calorimetry, DSC (see Fig. 13).

The low-temperature heat capacity is characterized by rather good accuracy and the results are usually available in the temperature range from liquid helium to the room temperature. Because of the limitation of the temperature function accepted in the present work (see Eqs 20 and 21) the description of the heat capacity was possible just above 250 K. Accordingly, the results of the adiabatic calorimetry were employed as two different kinds of measurements, the absolute entropy at 298.15 K that was estimated as an integral over all the temperature range and the upper part of the heat capacity curve (T > 250 K). The experimental entropies, $\{S_{ij}, z_{ij}, T_i\}$ are shown in Fig. 11 and Eqs (15) and (17) show the way how S_{ij}^{calc} can be computed from the model.

The precision of the heat capacity measured by DSC is not as good as for adiabatic calorimetry. Another problem is that at higher temperatures the oxygen adsorption/desorption can occur and interpretation of the results becomes rather difficult (see discussion in 93DEG/VOR). This was the reason why only the high-temperature heat capacities below 425 K were considered in the present work. In the original works, 90MAT/FUJ and 91SHA/OZE, the results are available up to 900 K.

It is impossible to obtain absolute values of the enthalpy and the Gibbs energy, and as was mentioned in Section 2, these properties are given for Reaction (3) (see Eqs. 2 and 14).

The enthalpy of formation of the $YBa_2Cu_3O_{6+z}$ phase has been measured in a number of laboratories by means of solution calorimetry (see Fig. 14 and Table 2) and, as one may expect, there is great scatter among the results. 95MON/POP have made a thorough review of calorimetry results where they have pointed out that the main problem responsible for the scatter between different laboratories is in impurities of the oxides used for the calorimetry (especially BaO that easily reacts with H_2O and CO_2 from the air). Then two sets of calorimetry experiments have been made based on rather a good correlation as follows. If authors have not paid attention to the purity of the samples, at least this question is not discussed in the paper (group H_b), then their results are quite different from those who have carefully discussed this problem (group H). Numerical results for the assessment have been taken from 95MON/POP where almost all results have been recalculated with the same set of auxiliary values.

There are few papers, 90AZA/SRE, 90FAN/JI, and 91SKO/PAS with the emf measurements of the Gibbs energy of formation from oxides. Because of the high-temperature nature of the method the results are available at the fixed oxygen partial pressure, *i.e.*, in the form of $\{\Delta_{ox}G_{ij}, T_{ij}, \ln p(O_2)_i\}$ (see Fig. 15). Only the results of 91SKO/PAS are in reasonable agreement with calorimetric enthalpies and entropies ($\Delta G = \Delta H - T\Delta S$). 91VOR/DEG2 have discussed all works and suggested that the disagreement in the case of 90AZA/SRE and 90FAN/JI can be explained by ambiguities in auxiliary values that are necessary to recalculate the experimental values to Reaction (3). As a result, group G which, in our view, we can rely upon contains just 91SKO/PAS and two other works are put into unreliable group G_b.

4. Simultaneous assessment under the linear error model

4.1. Formal task

Formally speaking, the task of the simultaneous assessment is to obtain a set of unknown parameters in Eq. (2) that gives the best description of the original experimental values described in Section 3 provided that thermodynamics properties of the oxides and oxygen are fixed (see Table 1). In other words, the system of equations (23) is to be solved in respect to vector Θ with the given set of experimental points $\{y_{ij}, u_{ij}, v_i\}$ (Eq. 22).

Thermodynamics adds some specifics to this rather general problem. First, function $y_{ij}^{calc}\{u_{ij}, v_i; \Theta\}$ is different for different experiments in which y_{ij} may mean completely different physical quantities. Second, the unknown parameters are defined in the Gibbs energy, they are inside the temperature functions $g_i(T)$, $a_i(T)$, $b_i(T)$ (see Eq. 21), but most equations are written for other thermodynamic properties that can be derived from the Gibbs energy by means some calculus. Because of that, the set of unknown parameters is the same for all the equations, even though equations may look quite differently. The lattice model also adds its own specifics, that is the most of the functions is not available in the closed form and thus the computation is heavily based on the numerical analysis.

Although computing $y_{ij}^{calc}\{u_{ij}, v_i; \Theta\}$ and thus solving the system (23) can not be named as routine, this is not the issue with current computer power at hand. The main problem lies in question what should be considered as the best description of the experimental points. Actually the number of unknowns in the system (23) is always greater that the number of equations because experimental errors ε_{ij} are also unknown. Therefore, there is an infinite number of solutions and which one should be taken as the best strongly depends on our considerations of errors. The latter will be referred as the error model and should not be confused with the thermodynamic model taken by itself.

The conventional approach is to employ the weight least squares (WLS) method, *i.e.*, to find such a solution that brings the sum of squares of the errors

$$ \text{SS} = \Sigma_{ij}\varepsilon_{ij}^2/W_{ij} = \boldsymbol{\varepsilon}' \, \mathbf{W} \, \boldsymbol{\varepsilon} \tag{27} $$

to the minimum. In matrix notation $\boldsymbol{\varepsilon}$ is the vector that comprises all the errors ε_{ij} from all the experiments (the number of elements $\Sigma_i N_i$) and $\mathbf{W}$ is the weight matrix that contains weights for each experimental point on its diagonal, $\mathbf{W} = diag\{W_{ij}\}$.

The problem that has got no clear answer in the weight least squares is how to assess the weights. The final solution certainly depends on the values of the accepted weights and a different set of weights would lead us to the different solution. Consequently, in the weight least squares method the task of the simultaneous assessment becomes mainly of that of the weight assignment. Mathematical statistics gives a guideline such that in order to obtain the reliable solution the weight matrix should be equal to inverse of the dispersion matrix of the error vector up to the factor

$$ \mathbf{W} = k \, \mathbf{D}(\boldsymbol{\varepsilon})^{-1} \tag{28} $$

The weight least squares based on Eq. (28) will be referred below as the strict weight least squares method. We can proceed from Eq. (28) to the weight least squares if all the errors ε_{ij} are postulated to be non-correlated (only in this case the dispersion matrix takes the diagonal form) and ratios between variances for all the errors are known *a priori*. Unfortunately, both statements are too restrictive for real-life applications. The variance ratio for experimental points is not known and there are clear evidences that at least some errors are correlated between each other because of the systematic errors. Then let us start with Eq. (28) and develop a more general approach than the weight least squares.

If variances are not known the maximum likelihood method allows us to determine both unknown parameters (vector $\boldsymbol{\Theta}$) and variances simultaneously by means of maximizing the likelihood function. This permits us to drop the requirement for variance ratios to be known. Provided all the errors are described by the multinormal distribution the maximum of the likelihood function coincides with the maximum of

$$L = - \ln \{\det[\mathbf{D}(\boldsymbol{\varepsilon})]\} - \boldsymbol{\varepsilon}' \, \mathbf{D}(\boldsymbol{\varepsilon})^{-1} \, \boldsymbol{\varepsilon} \tag{29}$$

If the error distribution is unknown, finding the maximum of Eq. (29) may be viewed as a heuristic procedure that gives not the worst estimates of the thermodynamics parameters and the components of the dispersion matrix (referred below as variance components). Some other methods for this task are also available (see 88RAO/KLE). Note that the weight least squares method is a special case of maximizing Eq. (29) when the variance components are known up to a constant, that is the maximum of (30) matches the minimum of (27) provided there are no other unknowns inside the dispersion matrix but the general factor (Eq. 28).

The linear error model

$$\varepsilon_{ij} = \varepsilon_{r,ij} + \varepsilon_{a,i} + \varepsilon_{b,i}(u_{ij} - u_i) \tag{31}$$

where

$$u_i = (\Sigma_j u_{ij})/N_i \tag{32}$$

has been recently introduced by 96RUD. It is assumed that the total experimental error ε_{ij} consists not only from the reproducibility error $\varepsilon_{r,ij}$ but also from two systematic errors $\varepsilon_{a,i}$ and $\varepsilon_{b,i}$. Both systematic errors are constant within the *i*-the experiment but they are assumed to change randomly among different experiments. The former systematic error accounts for the shift systematic error and latter for the tilt laboratory factor (tilt systematic error). Note that the linear error is a special case of so-called mixed models (see 88RAO/KLE).

The practical reason for introducing new two terms in Eq. (31) is that the results of the distinct experiments usually differ more between each other than the reproducibility error in a single experiment. Formally speaking, there is a statistically significant difference between distinct experiments, *i.e.*, the ratio of the corresponding sum of squares is more than Fisher's criterion allows. Then the systematic errors introduced above permit us to treat this situation by means of formal statistical procedures.

Eq. (31) was designed for one-dimensional tasks. Fortunately, it can be applied for the $YBa_2Cu_3O_{6+z}$ phase without any change even though functions $y^{calc}\{u, v\}$ that should be considered are at least two-dimensional. The reason is that all the measurements in the case of the $YBa_2Cu_3O_{6+z}$ phase are made by means of conventional approach when only one variable has been changed within a single experiment and thus they can be treated as pseudo-one-dimensional. Provided experimental physical chemistry switches to multidimensional experimental design, taking the modern analytical chemistry as a successful example, the linear error model may need to be modified.

The linear error model brings forth the dispersion matrix of experimental errors, $\mathbf{D}(\varepsilon)$ in the block-diagonal form (see details in 96RUD). Each block corresponds to the single experiment and its elements are functions of three variance components

$$D(\varepsilon_{r,ij}) = \sigma^2_{r,i}, \; D(\varepsilon_{a,i}) = \sigma^2_{a,i}, \; D(\varepsilon_{b,i}) = \sigma^2_{b,i} \tag{33}$$

It is worthy of noting that according to mathematical statistics (see Eq. 28) weights are related to variances of errors and not to the errors by themselves. In mathematical statistics, an error is considered to be a random quantity with the expected value equal to zero, and the variance is a property of this random quantity.

The considerations above allow us to set up a task as follows. For the given experimental points $\{y_{ij}, u_{ij}, v_i\}$, it is necessary to determine vector Θ with unknown parameters in the thermodynamic model and unknown variance components contained in the dispersion matrix simultaneously. The maximum likelihood method provides a framework to achieve this goal and also the criterion for the best solution for the system (23). The algorithm for maximizing Eq. (29) under the linear error model is described by 96RUD. Once more, the weight least squares is a special simplified case of the new general task that can be reached by equating the variances of systematic errors (and hence the systematic errors by themselves) to zero and supplying the ratio between variances of the reproducibility error *a priori*.

4.2. Expert conclusions

Let us stress the difference between experimental errors that can be treated statistically and mere mistakes of experimenters. If the expert conclusion is that there were some mistakes in carrying out the experiment, its results should not be averaged with other experiments because it is insensible to average "bad" and "good". In our case, several groups have been discarded before the statistical analysis based on our subjective opinion.

The experiments in groups Z_b, O_b, H_b and G_b have been assumed to be "bad" based on comparison with others in the alike category (see Section 3). During simultaneous assessment three other groups, T_z, P_b, and V have been found to strongly disagree with the results from different experimental categories and they also have been discarded. The question how to visualize the difference between results in different experimental categories is discussed in Section 5. We can speculate that adsorbed gases were responsible for high total pressures at lower temperatures measured by 94TAR/GUS (group V, see also Section 5) and that the indirect nature of the values presented in group T_z led to their shift by about 200 K in the temperature of tetragonal-orthorhombic transition (see Fig. 2). Yet, we can not say for sure what went wrong in the experiment on

oxygen partial enthalpy made by 89GER/PIC (group P_b) but the shape of the curve obtained (see Fig. 9) is in strong disagreement with our model and with the results in groups P and H.

It should be stressed once more that the results of groups Z_b, O_b, H_b, G_b, T_z, P_b, and V are in strong disagreement with the experiments included into the simultaneous assessment. If any experiment discarded by us happens to be the "true" one, then the results obtained in the present work should be reconsidered.

Three more groups, Z_g, O_g, and C_h have been also not included in the final assessment even though the results there are in reasonable agreement with the recommended solution. This means that the final solution does not depends principally whether these groups are included or not.

There were several reasons to exclude groups Z_g and O_g from the simultaneous assessment. First, the accuracy of these results that have been scanned from the figures are difficult to estimate because is not clear how these figures have been made (it is difficult to treat statistically errors made by the illustrator). Second, we believe that the authors that have failed to supply the results in the acceptable form should be somewhat punished (luckily we can afford this in the case of the $YBa_2Cu_3O_{6+z}$ phase). Generally speaking, the case of the $YBa_2Cu_3O_{6+z}$ phase is a very good example of the statement made by the IUPAC commission: "All will have had experience of cases when it has not been possible to decide on the relative merits of conflicting data because of insufficient reporting of uncertainties. Thus, years of work may be rendered useless by the failure of the authors to present his results fully or perhaps by failure to battle with editors for the essential space" (81OLO/ANG). Finally, if we would include these groups in the assessment, the statistical assumptions made below had become much more complicated.

The reason for excluding group C_h was mostly for cosmetic reasons. If the results of this group would left in the assessment this produced some sag in the description of the low-temperature heat capacities obtained by adiabatic calorimetry. As we think that these results are more accurate than those obtained by DSC, we have preferred the better description of the results in group C.

In the first step of expert conclusions described so far there were no difference between the weight least squares and the new approach described in the previous section. The difference starts in the next step when it is necessary to ascribe weights to the experimental points that have been included in the simultaneous assessment.

In order to utilize either the weight least squares or maximum likelihood method, some hypotheses should be formulated about the error dispersion matrix. Note that because of Eq. (28) the terms "dispersion matrix" and "weight matrix" are considered sometimes as synonyms in the present work. In many works the weights are just chosen by expert without any use of Eq. (28). We will call this as the informal weight least squares method. In the last case, the expert has to specify the numerical values of the weights (the ratios between variances) for all the experimental points. This usually takes a lot of meditating. The statement "this work is better than that one" is relatively easy to make but the numerical assertion "this work is better by two and half times that that one" is certainly not that straightforward for the human being.

The maximum likelihood method allows the expert to limit herself by qualitative conclusions only. The expert set the structure of the error dispersion matrix and all the numerical values will be estimated during maximizing the likelihood function. Let us see how this idea was implemented in the present work.

First, all the experiments have been divided into the groups of the same quality as was discussed in Section 3 (see Table 3) and some of groups have been discarded as explained above. Certainly, some meditating was inevitable during this process but because of the qualitative nature of this procedure the considerations can be explained easier than in the informal weight least squares.

Our final expert conclusion was that we have ten miscellaneous groups of experiments (T_z, X, Z, O, N, P, S, C, H, G) and that all of them seem to have about the same quality. Now this statement is necessary to express in the formal manner. First, the variance of the reproducibility error can be assumed to be the same within each group that gives ten unknown variances. The statement of the same quality of the experiments in these groups can not be applied to the reproducibility variances because we can not ever think that there is any relationship between the reproducibility variances in different groups.

The problem now is that the experimental values that have been put into the assessment can not be described within their reproducibility error. If we put the solution within the reproducibility error for one group then it for sure will go beyond the reproducibility error for another group. Then Eq. (31) allows us to make the next step and to explain this fact by introducing the systematic errors and to reformulate the statement of the same quality for the different groups as the principle of the like compromise. This is that the two rations

$$\gamma_{a,i} = \sigma^2_{a,i}/\sigma^2_{r,i}, \; \gamma_{b,i} = \sigma^2_{b,i}/\sigma^2_{r,i} \tag{34}$$

are assumed to be the same for all the groups included in the simultaneous assessment. To clarify this principle, let us start with the first ratio, $\gamma_{a,i}$.

Under the linear error model the total error is considered to consist from three terms. The first is the reproducibility error and the second is the shift systematic error. The latter allow us to model the calibration error because now one can say that the experimenter has made the common error while preparing the apparatus. This error was constant for all the points in this experiment and then during the measurement procedure the reproducibility error was added at each point. Statistically speaking, both errors are considered to be random but they are characterized by different variances, reproducibility variance and shift systematic variance. The sift systematic variance should be different for different groups because it is dimensional quantity and the dimension is different. However, ratio $\gamma_{a,i}$ shows the shift systematic variance measured by the reproducibility variance in the i-th group and thus it is dimensionless. Then, when we speak about the same quality for the experiments in different groups this may well mean that ratio $\gamma_{a,i}$ is the same for these groups.

The situation is analogous with the second ratio, $\gamma_{b,i}$. However there is some small additional problem here because $\gamma_{b,i}$ is still dimensional. The third term in Eq. (31) as the second one is also tied with the systematic error but its nature is different. It is such an systematic error that forces the measured curve to tilt from the true behavior. As a result the tilt systematic variance is associated with the unit length of the controlled variable u,

and ratio $\gamma_{b,i}$ has the dimension equal to the inverse of the u variable. Then before we say that ratio $\gamma_{b,i}$ is the same for different groups it is necessary to compare unit lengths of different controlled variables. This was done by choosing typical ranges of the controlled variable as 1000 K for temperature, as 10 for ln $p(O_2)$, and as 1 for index z and by somewhat arbitrary equating these ranges between each other.

The assumptions made above gives twelve unknowns in the error dispersion matrix (ten for reproducibility variances and two for the ratios in Eq. 34). The maximum likelihood method allow us to leave the variance components as unknowns in the dispersion matrix and to estimate them during the maximization of (29) simultaneously with estimating unknown parameters in Eq. (2).

4.3.   Maximizing the likelihood function

Another reason for meditating during the simultaneous assessment is a choice of the number of unknown parameters. Actually, Eq. (2) is the expansion in series and before maximizing Eq. (29) the number of terms in the two sums is to be defined. The same also concerns Eq. (21) employed in the present work as the temperature function within Eq. (2). A typical solution to this problem is to perform the assessment several times when the number of unknowns is changed. Two criteria have been used to choose the optimal number of unknown parameters: the best description of the experimental points and, at the same time, the conformity of the thermodynamic properties obtained to the general trends of similar materials. Also during the addition of new unknowns, the attention has been paid not to make the whole task ill-behaved.

In the previous assessment of 93DEG/VOR, the approximation for the heat capacity, $\Delta_{ox}C_{px} = 0$ has been utilized. This means that just two unknown parameters, A and B have been left in each temperature function, $g_i(T), a_i(T), b_i(T)$ there. However, Fig. 12 and Fig. 13 display that the experimental heat capacity is higher than predicted by this approximation and one of the goals in the present assessment was to obtain the better description of the heat capacity. To this end, additional unknowns are to be introduced in the temperature functions in addition to A and B. Yet, the number of these additional unknowns happens to be rather limited. It happened to be impossible to put new unknowns in each temperature function because this would lead to unphysical behavior of the heat capacity.

After many attempts, we have preferred to introduce new variables C and D in temperature function $g_2(T)$ only. This means that approximation $\Delta_{ox}C_{px} = 0$ has been changed to $\Delta_{ox}C_{px} = k(T)\,z$. The more realistic approximations will be possible after new experimental values on the heat capacity for the compositions close to $z = 0$ appear.

In the second sum of Eq. (2) the only the first term, $b_1(T)$ has been left. The unknowns in the second sum depend mainly on the tetragonal-orthorhombic phase transition and occupancies in the oxygen sublattices. It happens that one term is enough for the description of these values. The addition of other terms made the task ill-behaved.

Fig. 16 explains our choice for the number of terms in the first sum of Eq. (2). As the number of terms grows the maximum likelihood function after sharp rise comes to the

saturation, and simultaneously, the opposite is held for the ratios, $\gamma_{a,i}$ and $\gamma_{b,i}$. Based on this fact, the two terms in the first sum have been assumed to be optimal for the description of the $YBa_2Cu_3O_{6+z}$ thermodynamic properties.

Finally, we have twelve unknown parameters in the Gibbs energy in addition to ten unknown variance components defined in the previous section. All of them have been determined by maximizing Eq. (29) numerically (see 96RUD for the description of the algorithm). The final values of variance components are presented in Table 4, the values of parameters are in Table 5. Fig. 1 to Fig. 15 compare the solution obtained with the original experimental points and Fig. 17 presents the phase diagram of the $YBa_2Cu_3O_{6+z}$ phase computed from the assessed Gibbs energy. Some less usual pictures (Fig. 18 to Fig. 27) are discussed in the next sections. The correlation matrix for the parameters obtained is given in Table 6. It is important for estimating the variance of the predicted thermodynamic properties at given external conditions. Finally, some thermodynamic properties of the $YBa_2Cu_3O_{6+z}$ phase are tabulated in Table 7. A small program Y123.EXE working under WINDOWS 95 and WINDOWS NT to compute the thermodynamic properties on the fly is available from the authors (http://www.chem.msu.su/~rudnyi/Y123/welcome.html).

5.   Visualizing the quality of the fit

Recently 93ALC/ITK have emphasized the necessity for the intelligent appearance of the measurements in the graphical form in the excellent paper devoted to O. Kubaschewski. We agree completely with 93ALC/ITK that a single statistical criterion can not replace the analysis of the figures.

Fig. 1 to Fig. 15 are typical examples of figures when the fitted curves are compared with the experimental points. The problem is that there are too many figures and it would be good to make some digest. Also note that the scale of the figures is low and. As a result, we can see large effects only, and it is difficult to follow fine details of the data description.

Plotting deviates, *i.e.*, the differences y_{ij} - $y_{ij}^{calc}\{u_{ij}, v_i; \Theta\}$ allow us to sharply enhance the scale and to put more values on the same graph. Fig. 18 and Fig. 19 demonstrate this statement with an example of two groups, Z_g and O_g which were not included in the assessment. It would be necessary at least several figures in each group to plot all the experimental points in reasonable fashion by means of the conventional figures. Note that because of the enhanced scale, at first glance the scatter may look as rather bad but actually it is about 0.05 in the value of index z and about 0.8 in the value of ln $p(O_2)$. The latter value means that the difference in the oxygen partial pressures is two times that should not be considered as bad because the absolute value of the oxygen partial pressure was changed by six orders of magnitude and the method employed were rather diverse.

It is possible to go further and to plot deviates normalized by the square root of the reproducibility variance, $[y_{ij}$ - $y_{ij}^{calc}\{u_{ij}, v_i; \Theta\}]/\sigma_{r,ij}$ (see Fig. 20). This allows us to put the results of heterogeneous experiments on the same figure and to compare them between each other because now the deviates are dimensionless as they are measured by their standard deviation of the reproducibility. Fig. 20 can be named as a statistical picture of

the $YBa_2Cu_3O_{6+z}$ phase because it contains all the experimental points that have been processed simultaneously.

Because of the huge number of experimental points, Fig. 18 to Fig. 20 are too messy. Now it is difficult to find out a particular experiment. Fig. 20 is more of esthetic than practical value (especially when it is made in colors). Then the linear error model suggests us a new type of the graph when each experiment is represented by a single point. The idea is that a typical behavior of the deviates in a single experiment can be described by a line and hence the experimentally measured values are shifted and tilted over the final fitted curve. Hence it is possible to plot the tilt *vs.* shift to see the extent of overall agreement among all the experiments. Again, the tilt and shift is to be normalized by the standard deviation of the reproducibility to make the comparison of different types of experiments possible. More details about this type of a graph are given elsewhere (96RUD, 97KUZ/USP, and 97RUD).

Fig. 21 and Fig. 22 present this type of the figure for two solutions, recommended in the present work (ML) and from the previous assessment by 93DEG/VOR. This gives us an overview of the description of all the experiments. It is clearly seen that in the present assessment two things have been improved considerably: the description of the high pressure results of 92CON/KAR and the heat capacity.

Now let us take the paper of 94TAR/GUS as an example to demonstrate how it is possible to compare different type of experiments during the simultaneous assessment. The problem is that in the beginning of the assessment is not quite clear what experiments agree between each other and what do not. Our approach was to start by including all the experiments, to draw the graphs similar to explained above and then to take a decision. During this process we have seen that the results of 94TAR/GUS are in great disagreement with many papers on the oxygen partial properties and one of the tricks that helped us significantly was to play a game "what if". The disagreement can be seen from Fig. 23 where our solution is shown with respect to the experimental points. If we include the results of 94TAR/GUS with non-zero weight the description of their experiments gets much more reasonable (solution TAR in Fig. 23). However the better description for the 94TAR/GUS means much worse description for other experiments that can be clearly seen from Fig. 24. It shows that if we say that 94TAR/GUS is right then it would mean that many others are wrong, and we have preferred the opposite conclusion. It is worthy of noting that the experimental consideration also played not the last role in our conclusion: it may well be that the adsorbed gases and not the oxygen led to high total pressure at low temperatures in the experiments of 94TAR/GUS.

6. Comparison with the weight least squares

The main difference of the present assessment from the conventional approach lies in introducing the linear error model with two systematic errors. Let us now discuss what the practical difference this brought about. To this end, another solution have been found when the variances of systematic errors have been zeroed and the variance of the reproducibility error was assumed to be equal to that obtained in solution ML. This implements the strict weight least squares method when the weight is equal to the inverse

of the reproducibility variance. Note that the reproducibility variances found by maximum likelihood method under the linear error model should be close to the pool variance of reproducibility for a particular group of experiments. The solution, referred as WLS is shown in Fig. 1 to Fig. 15. It is also compared with solution ML in Fig. 25 to Fig. 27.

First, it is possible to state that the description of the original experimental points by both solutions is rather similar. The overall description is even a bit better in solution WLS. This can be seen while Fig. 25 is compared with Fig. 21: a circle of experiment marks is a bit smaller in the case of solution WLS.

However, there are some subtle effects that allow us to declare solution WLS as worse in comparison with ML. In the case of the $YBa_2Cu_3O_{6+z}$ phase it is possible to distinguish between the overall description (for example, the sum of weighted squares) and the description of the function behavior, and our conclusion is that while the former is better for solution WLS the latter is better for solution ML. Fig. 26 and Fig. 27 demonstrate this with an example of experiments from group Z. The deviates in group Z are smaller in Fig. 27 (solution WLS) than in Fig. 26 (solution ML). However the deviates for a particular experiment in Fig. 27 possess S-form that can be seen for most series. Therefore, one can say that the function behavior is described better in Fig. 26 even though the overall agreement there is a bit worse. The same can be also said about other groups.

The function behavior in groups Z and O determine the condition for the tetragonal-orthorhombic phase transition. As a result, we believe that the description of the phase transition is better in solution ML. This may be confirmed by the predicted phase diagram of the $YBa_2Cu_3O_{6+z}$ phase (see Fig. 17). The phase diagram that follows from solution ML is rather close to that obtained in the previous assessment of 93DEG/VOR and to what may be expected from many structural and theoretical studies. The phase diagram predicted by solution WLS is quite different and we believe that it is physically unreasonable.

Pragmatically speaking, solutions ML and WLS differ by variances of systematic errors: these variances were assumed to be zero in the last case and were considered to be unknowns in the former case. This is responsible for the effect described above. When the weights have been assigned to the experimental points based on the reproducibility variance in the strict weight least squares, the number of points in a particular experiment and the range of the controlled variable automatically have been used as additional weights while the results of the different experiments have been processed altogether.

From the first glance, employing number of experimental points as a weight at otherwise equal conditions seems not to be a bad idea. Yet, if we take into account systematic errors, this should be carefully reconsidered. A systematic error is what was constant in a particular experiment. Then the number of experimental points should not lower the systematic error. Let us imagine that there are two experiments with the number of points 10000 and 10 accordingly. Provided there were systematic errors that are bigger than the reproducibility error in each experiment, ascribing weights equal to the numbers of points seems not to be a good solution. The large number of points lead us to small reproducibility error of the mean but this does not count for systematic error. Then from a viewpoint of the like compromise the systematic errors may be assumed to be the same in

both experiments, and because they do not depend on the number of points it is necessary to average the two means with weights equal to one.

There is no other way in the weight least squares to lessen the number of points in a particular experiment than to switch the informal weight least squares. Here, the weight is considered to be an expert opinion about the quality of the experiment and Eq. (28) is thrown out. This is always possible but lead us to a lot of meditating because the solid ground to take the decision is already lost.

The inclusion of the systematic errors in the error model allow us to lessen the effective number of experimental points formally because of the block-diagonal structure of the dispersion matrix in this case. After the total error has been separated to the reproducibility error and the systematic errors, the structure of Eq. (29) leads to the following fact. For the likelihood function under the linear error model to reach maximum, it is more beneficial to make the reproducibility variance as low as possible even if this would require some increase in the variances of systematic errors. This explains why the better description of the function behavior has been achieved in solution ML.

7.   Conclusion

The main practical result of the present work is a new set of parameters for the Gibbs energy of the $YBa_2Cu_3O_{6+z}$ phase which is the key phase for thermodynamics of the Y-Ba-Cu-O quaternary system. Most results for other phases in this system include equilibria with the $YBa_2Cu_3O_{6+z}$ phase, and thus, the assessment of the whole system depends heavily on thermodynamic values accepted for the $YBa_2Cu_3O_{6+z}$ phase.

Even though the $YBa_2Cu_3O_{6+z}$ phase has attracted a lot of attention in the last decade there are some "white spots" left. First, this concerns the area about room temperature where the phase diagram shown in Fig. 17 may well be not quite correct. The recent results suggest existence of so called superstructures at these temperatures, and the model employed in the present work does not allow us to describe superstructures at all. Another direction for the improvement of the model is the high pressure region (more than 10^8 Pa) where it is impossible to neglect the hydrostatic pressure. At the same time, we believe that the thermodynamic properties at high temperatures and at moderate pressures are well-studied now, that our model describes these experimental values adequately, and that this description will not be changed significantly in the foreseeable future.

Besides concrete numbers, there are some methodological points to discuss that are of general interest in thermodynamic assessment. Steps to be taken in simultaneous assessment are as follows:

1) Collecting a database of experimental values.

2) Developing a thermodynamic model.

3) Formulating expert conclusion.

4) Computing unknown parameters and optionally unknown variance components.

Let us see what improvements can be achieved here by employing the linear error model.

First, the whole process can not be done in a single sequence and in practice the thermodynamic assessment is somewhat a circular movement over these steps until the full satisfaction of the assessor or probably more often until the time or/and money limit has been reached. Second, this process can not be completely formalized and the strategic decisions for the final model and the quality of the experimental works are always subjective (see 93ALC/ITK for a good discussion on this matter). While keeping this in mind, we enlarge on the last two steps when the model and the experiments to be processed are already chosen.

The starting point for the expert conclusions is the error model that determine the structure of the dispersion and hence weight matrix. It is the error model that gives the solid background for averaging the experimental values. In the conventional approach, the error model includes just a reproducibility error and, as a result, the weight (dispersion) matrix has the diagonal form. Then an expert should supply the numerical values of all the weights. Sometimes the expert proceeds from Eq. (28) with the use of some estimates of reproducibility variances, but more often she just weighs somehow the quality of experimental points.

However if we study deviates (see Fig. 18 to Fig. 20, Fig. 26 and Fig. 27) we can see that the total error can not be modeled as the reproducibility scatter only, and this is quite common for all the real experimental measurements. The results of a single experiment are not scattered over the fitted curve randomly but rather they are shifted and tilted systematically. Then, if we need reliable results we have got to explain this behavior, or otherwise the experimental values will be processed under a wrong error model.

The linear error model accepted in the present work is a first step in explaining the regular behavior of the deviates. It is said that the results are shifted and tilted because of the systematic errors, and, in our view, this is quite conceivable. Definitely, the linear error model is also some approximation of the real picture, and it is possible to introduce more sophisticated error models (see, for example, 88RAO/KLE). Yet, the linear error model allows us to catch the main effects in the trend of the deviates which can not be ignored and to leave some more subtle effects to the future development.

Pragmatically speaking, the linear error model allow us to switch to the non-diagonal dispersion and hence weight matrix. This, in turn, gives us some appropriate tool to influence the number of experimental points in different experiments as discussed in the previous section. The comparison of the two solutions, ML and WLS shows that because of treating the systematic errors as the reproducibility ones the weight least squares have brought such a solution when the description of the function behavior is inappropriate.

Another difference of our approach with the conventional one is in estimating variance components. It is possible to say that in the weight least squares the estimation of the variance components is expert's responsibility and in our approach they are estimated by means of the maximum likelihood method simultaneously with unknown parameters. This means that expert's work gets a bit easier because the expert can express her opinion in the qualitative form.

The importance of graphics could not be overestimated. It is impossible to produce a reliable assessment by any method without viewing what the agreement between

experimental points and the fitted curve looks like in figures. In the present work three types of figures have been employed and from our experience we can state that the best results can be achieved by a combination of all three graph types. Each type shows up its own specific information that is difficult to figure out from another types of graphs.

Finally, the advancement of Internet permits archiving the materials that are necessary for the assessment in the public domain. Our materials including the database of all the experimental values and the optimization software (for WINDOWS 95 and WINDOWS NT) are available from our site, http://www.chem.msu.su/~rudnyi/Y123/welcome.html. After all, if you are not satisfied with our set of parameters you are welcome to make your own.

8. Acknowledgment

9. References

81OLO/ANG   Olofsson, G., Angus, S., Armstrong, G.T., Kornilov A.N. J. Chem. Thermodynamics, 13, 603 (1981).

85BER/BRO   Berman, R.G., Brown, T.H., Contrib. Mineral. Petrol. 89, 168 (1985).

87BRY/GAL   O'Bryan, H.M., Gallagher, P.K., Adv. Ceram. Mater. 2, 640 (1987).

87EAT/GIN   Eatough, M.O., Ginley, D.S., Morosin, B., et al., Appl. Phys. Let. 51, 367 (1987).

87FIO/GUR   Fiory, A.T., Gurvitch, M., Cava, R.J., et al., Phys. Rev. B 36, 7262 (1987).

87JOR/BEN   Jorgensen, J.D., Beno, M.A., Hinks, D.G., et al., Phys. Rev. B 36, 3608 (1987).

87KIS/SHI   Kishio, K., Shimoyama, J., Hasegawa, T., et al., Jpn. J. Appl. Phys. 26, L1228 (1987).

87KUB/NAK   Kubo, Y., Nakabayashi, Y., Tabuhi, J., et al., Jap. J. Appl. Phys., Part 2 26, L1888 (1987).

87SAL/KOE   Salomons, E., Koeman, N., Brouer, R., et al., Solid State Commun. 64, 1141 (1987).

87SCH/HIN   Schuller, I.K., Hinks, D.C., Beno, M.A., et al., Solid State Commun. 63, 385 (1987).

87STR/CAP   Strobel, P., Capponi, J.J., Marezio, M., et al., Solid State Commun. 64, 513 (1987).

87TAK/UCH   Takayama-Muromachi, E., Uchida, Y., Yukino, K., et al, Jpn. J. Appl. Phys, 26, L665 (1987).

87YUK/SAT   Yukino, K., Sato, T., Ooba, S., et al., Jpn. J. Appl. Phys. 26, L869 (1987).

88GAV/GOR   Gavrichev, K.S., Gorbunov, V.E., Konovalova, I.A., et al., Izv. AN SSSR, Neorg. mater. 24, 343 (1988).

88IKE/NAG   Ikeda, K., Nagata, M., Ishihara, M., et al., Jpn. J. Appl. Phys., 27, L202 (1988).

88KOG/NAK   Kogachi, M., Nakanishi, S., Nakahigashi, K., et al., Jap. J. Appl. Phys. 27, L1228 (1988).

88MEU/RUP   Meuffels, P., Rupp, B., Porschke, E., Phys. C 156, 441 (1988).

88MOR/SON   Morss, L.R., Sonnenberger, D.C., Thorn, R.J., Inorg. Chem. 27, 2106 (1988).

88RAO/KLE   Rao, C.R., Kleffe, J. Estimation of variance components and applications, North-Holand, Amsterdam, (North-Holland Series in Statistics and probability, v.3), 1988, 370 pp.

88SHE/CHU   Sheiman, M.S., Churin, S.A., Kamedova, G.P., et al., Tezisy dokladov XII Vsesoyuznoi konferentsii po khimicheskoi termodinamike i kalorimetrii (XII All-union conference on chemical thermodynamics and calorimetry, Abstracts), Gorkii, v. 1, p. 140 (1988).

88SPE/SPA   Specht, E.D., Sparks, C.J., Dhere, A.G., et al., Phys. Rev. B 37, 7426 (1988).

88TOU/MAR   Touzelin, B., Marucco, J.F., J. Less-Common Metals 144, 283 (1988).

88WAN/LI   Wang, H., Li, D.X., Thomson, W.J., J. Amer. Cer. Soc. 71, C463 (1988).

88YAM/TER   Yamaguchi, S., Terabe, K., Saito, A., et al., Jap. J. of Appl. Phys., Part 2 27, L179 (1988).

89BOR/NOL   Bormann, R., Nolting, J., Appl. Phys. Let. 54, 2148 (1989).

89BRY/GAL   O'Bryan, H.M., Gallagher, P.K., Solid State Ionis 32/33, 1143 (1989).

89GER/PIC   Gerdanian, P., Picard, C., Marucco, J.F., Physica C 157, 180 (1989).

89GRU/PIV   Grunin, V.S., Pivovarov, M.M., Patrina, I.B., et al., Dokl. Acad. Nauk SSSR 307, 143 (1989).

89JUN/ECK   Junod, A., Eckert, D., Triscone, G., et al., Phys. C 159, 215 (1989).

89LIN/HUN   Lindemer, T.B., Hunley, J.F., Gates, J.E., et al., J. Am. Ceram. Soc. 72, 1775 (1989).

89MEU/NAE   Meuffels, P., Naeven, R., Wenzl, H., Phys. C 161, 539 (1989).

89PAR/NAV   Parks, M.E., Navrotsky, A., Mocala, K., et al., J. Sol. St. Chem. 79, 53 (1989).

89TET/TAN   Tetenbanm, M., Tani, B., Czech, B., et al., Physica C 158, 377 (1989).

89VER/BRU   Verweij, H., Bruggink, W.H.M., J. Phys. Chem. Solids 50, 75 (1989).

90AZA/SRE   Azad, A.M., Sreedharan, O.M., Supercond. Sci. Technol. 3, 159 (1990).

90DEG   Degtyarev, S.A., Sverkhprovodimost: Fiz., Khim., Tech. 3, 115 (1990).

90DEG2   Degtyarev, S.A., Sverkhprovodimost: Fiz., Khim., Tech. 3, 130 (1990).

90FAN/JI   Fan, Z., Ji, C.J., Zhao, Z., J. Less-Com. Met. 161, 49 (1990).

90FUE/IDE   Fueki, K., Idemoto, Y., Ishizuka, H., Phys. C 166, 261 (1990).

90MAT/FUJ   Matsui, T., Fujita, T., Naito, K., et al., J. Solid State Chem. 88, 579 (1990).

90MER/DEG   Merzhanov, I.A., Degtyarev, S.A., Sverkhprovodimost: Fiz., Khim., Tech. 3, 125 (1990).

90SHA/WES   Shaviv, R., Westrum, E.F., Brown, R.J.C., et al., J. Chem. Phys. 92, 6794 (1990).

91ATA/HON   Atake, T., Honda, A., Kawaji, H., Physica C 190, 70 (1991).

91GAR/RAI   Garzon, F.H., Raistrick, I.D., Ginley, D.S., et al., J. Mater. Res. 6, 885 (1991).

91LEE/LEE   Lee, B.J., Lee, D.N, J. Am. Ceram. Soc. 74, 78 (1991).

91SCH/HAR   Schleger, P., Hardy, W.N., Yang, B.X., Physica C 176, 261 (1991).

91SHA/OZE   Sharpataya, G.A., Ozerova, Z.P., Konovalova, I.A., et al., Neorg. Mater. 27, 1674 (1991).

91SKO/PAS   Skolis, Yu.Ya., Pashin, S.F., Kitsenko, S.V., et al., Tezisy dokladov 13 Vsesoyuznoi konferentsii po khimicheskoi termodinamiki i kalorimetrii (All-union conference on chemical thermodynamics and calorimetry, Abstracts), Krasnoyarsk, v. 1, p. 62 (1991).

91VOR/DEG   Voronin, G.F., Degterov, S.A., Physica C 176, 387 (1991).

91VOR/DEG2   Voronin, G.F., Degtyarev, S.A., Skolis, Yu.Ya., Dokl. Acad. Nauk SSSR 319, 899 (1991).

92CHO/KAN   Choy, J.H., Kang, S.G., Choi, Q.W., et al., Materials Letters 15, 156 (1992).

92CON/KAR   Conder, K., Karpinski, J., Kaldis, E., et al., Physica C 196, 164 (1992).

92IDE/TAK   Idemoto, Y., Takahashi, J., Fueki, K., Physica C 194, 177 (1992).

92MAT/JAC   Mathews, T., Jacob, K.T., Metallurgical Transactions A 23A, 3325 (1992).

92ZHO/NAV   Zhou, Z.G., Navrotsky, A., J. Materials Research 7, 2920 (1992).

93ALC/ITK   Alcock, C.B., Itkin, V.P., J. Phase Equilibria 14, 409 (1993).

93DEG/VOR   Degtyarev, S.A., Voronin, G.F., Zhurn. Fiz. Khim. 67, 1351 (1993).

93MAT/POP   Matskevich, N.I., Popova, T.L., Titov, V.A., et al., Zhurn. Fiz. Khim. 67, 1342 (1993).

93PLE/ALT   Plewa, J., Altenburg, H., Hauck, J., Z. Metallkunde, 84, 652 (1993).

93PRI/ZIN   Prisedskii, V.V., Zinchenko, O.V., Lotar', E.V., Dokl. Acad Nauk Ukrainy 4, 130 (1993).

94KIM/GAS   Kim, J.S., Gaskell, D.R., J. Amer. Ceram. Soc. 77, 753 (1994).

94MON/POP   Monaenkova, A.S., Popova, A.A., Zaitseva, N.V., et al., Zhurn. Fiz. Khim. 68, 603 (1994).

94TAR/GUS   Tarasov, I.V., Gus'kov, V.N., Lazarev, V.B., Neorg. Mater. 30, 1588 (1994).

95HEN/ZHE   Hengzhong, Z., Zheng, F., Pingmin, Z., et al., J. Sol. Chem. 24, 565 (1995).

95MON/POP   Monaenkova, A.S., Popova, A.A., Zaitseva, N.V., Zhurn. Fiz. Khim. 69, 1543 (1995).

96BOU/HAC   Boudene, A., Hack, K., Mohammad, A., Neuschutz, D., et al, High Temp. Mater. Sci., 35, 159 (1996).

96RUD   Rudnyi, E.B., Chemometrics Intel. Lab. Systems 34, 41 (1996).

97KUZ/USP   Kuzmenko, V.V., Uspenskaya, I.A., Rudnyi, E.B., Bull. Soc. Chim. Belges N 5 (1997).

97RUD   Rudnyi, E.B., Chemometrics Intel. Lab. Systems 36, 213 (1997).

97VOR/USP   Voronin, G.F., Uspenskaya, I.A. Zh. Fiz. Khim. (1997).

Table 1. Auxiliary thermodynamic properties of oxides employed in the present work (according to 97VOR/USP)[a]

oxide	$\Delta_fH^o{}_{298}$ kJ·mol^{-1}	A	B	C	D	E	F
Y_2O_3	-1919.4	-30047.83	954.1052	-146.996	-2120.104	737146.5	-12441857
BaO	-548.0	-5092.968	463.41195	-72.028	-1858.564	0	-9963433
CuO	-161.7	-5669.132	477.64762	-69.785	-1801.184	61609	0
O_2	0	-1776.280	132.54252	-44.978	-1294.168	0	-13651002

[a] the parameters from A to F allow us to compute the standard Gibbs energy of the oxide (p^o = 101325 Pa) according to Eq. 21 in J·mol^{-1} in the temperature interval from 250 K to 1300 K, all other thermodynamic properties of the oxide can be obtained by means of well-known thermodynamic relationships.

Table 2. Experimental results available for the assessment of the $YBa_2Cu_3O_{6+z}$ phase thermodynamics

Code	Set of values	N_i	Inc.[a]	v_i[b]	Method[c]	Reference
TB1	$\{T_{ij}, \ln p(O_2)_{ij}\}$	5	+	n/a	XRD	87BRY/GAL
TE	$\{T_{ij}, \ln p(O_2)_{ij}\}$	2	+	n/a	XRD	87EAT/GIN
TF	$\{T_{ij}, \ln p(O_2)_{ij}\}$	10	+	n/a	resistivity	87FIO/GUR
TK	$\{T_{ij}, \ln p(O_2)_{ij}\}$	5	+	n/a	TGA	87KUB/NAK
Ts	$\{T_{ij}, \ln p(O_2)_{ij}\}$	1	-	n/a	XRD	87SCH/HIN
TT	$\{T_{ij}, \ln p(O_2)_{ij}\}$	2	+	n/a	TGA, XRD	87TAK/UCH
TY	$\{T_{ij}, \ln p(O_2)_{ij}\}$	1	+	n/a	XRD	87YUK/SAT
To	$\{T_{ij}, \ln p(O_2)_{ij}\}$	2	+	n/a	XRD	88KOG/NAK
Tp	$\{T_{ij}, \ln p(O_2)_{ij}\}$	5	+	n/a	XRD	88SPE/SPA
Tu	$\{T_{ij}, \ln p(O_2)_{ij}\}$	4	+	n/a	XRD	88TOU/MAR
TW	$\{T_{ij}, \ln p(O_2)_{ij}\}$	4	+	n/a	XRD	88WAN/LI
TB2	$\{T_{ij}, \ln p(O_2)_{ij}\}$	1	+	n/a	XRD	89BRY/GAL
TM1	$\{T_{ij}, z_{ij}\}$	7	-	n/a	resistivity	88MEU/RUP
TM2	$\{T_{ij}, z_{ij}\}$	13	-	n/a	resistivity	89MEU/RUP
XJ0	$\{x_{ij}, T_{ij}, \ln p(O_2)_i\}$	16	+	p = 1	ND	87JOR/BEN
XJ1	$\{x_{ij}, T_{ij}, \ln p(O_2)_i\}$	7	+	p = 0.2	ND	87JOR/BEN
XJ3	$\{x_{ij}, T_{ij}, \ln p(O_2)_i\}$	7	+	p = 0.02	ND	87JOR/BEN
XI1	$\{x_{ij}, T_{ij}, \ln p(O_2)_i\}$	9	+	p = 0.2	XRD	88IKE/NAG
ZJ0	$\{z_{ij}, T_{ij}, \ln p(O_2)_i\}$	17	-	p = 1	ND	87JOR/BEN
ZJ1	$\{z_{ij}, T_{ij}, \ln p(O_2)_i\}$	7	-	p = 0.2	ND	87JOR/BEN
ZJ3	$\{z_{ij}, T_{ij}, \ln p(O_2)_i\}$	7	-	p = 0.02	ND	87JOR/BEN
ZI1	$\{z_{ij}, T_{ij}, \ln p(O_2)_i\}$	10	-	p = 0.2	TGA	88IKE/NAG
Zt0	$\{z_{ij}, T_{ij}, \ln p(O_2)_i\}$	7	-	p = 1	TGA	87STR/CAP
Zt1	$\{z_{ij}, T_{ij}, \ln p(O_2)_i\}$	7	-	p = 0.25	TGA	87STR/CAP
Zt3	$\{z_{ij}, T_{ij}, \ln p(O_2)_i\}$	7	-	p = 0.050	TGA	87STR/CAP
Zt4	$\{z_{ij}, T_{ij}, \ln p(O_2)_i\}$	7	-	p = 0.01	TGA	87STR/CAP
Zt6	$\{z_{ij}, T_{ij}, \ln p(O_2)_i\}$	4	-	p = 0.001	TGA	87STR/CAP
ZS0	$\{z_{ij}, T_{ij}, \ln p(O_2)_i\}$	35	-	p = 0.74	TGA	88SPE/SPA
ZS1	$\{z_{ij}, T_{ij}, \ln p(O_2)_i\}$	8	-	p = 0.36	TGA	88SPE/SPA
ZT0	$\{z_{ij}, T_{ij}, \ln p(O_2)_i\}$	8	-	p = 1	TGA	88TOU/MAR
ZT1	$\{z_{ij}, T_{ij}, \ln p(O_2)_i\}$	6	-	p = 0.2	TGA	88TOU/MAR
ZY0	$\{z_{ij}, T_{ij}, \ln p(O_2)_i\}$	26	-	p = 1	TGA	88YAM/TER
ZY0a	$\{z_{ij}, T_{ij}, \ln p(O_2)_i\}$	9	-	p = 0.7	TGA	88YAM/TER
ZY1	$\{z_{ij}, T_{ij}, \ln p(O_2)_i\}$	9	-	p = 0.4	TGA	88YAM/TER
ZY1a	$\{z_{ij}, T_{ij}, \ln p(O_2)_i\}$	29	-	p = 0.2	TGA	88YAM/TER
ZY3	$\{z_{ij}, T_{ij}, \ln p(O_2)_i\}$	24	-	p = 0.053	TGA	88YAM/TER
ZY4	$\{z_{ij}, T_{ij}, \ln p(O_2)_i\}$	26	-	p = 0.013	TGA	88YAM/TER
ZY5	$\{z_{ij}, T_{ij}, \ln p(O_2)_i\}$	24	-	p = 0.005	TGA	88YAM/TER
ZY6	$\{z_{ij}, T_{ij}, \ln p(O_2)_i\}$	9	-	p = 0.0022	TGA	88YAM/TER
ZY7	$\{z_{ij}, T_{ij}, \ln p(O_2)_i\}$	6	-	$p = 3 \cdot 10^{-4}$	TGA	88YAM/TER
ZB8	$\{z_{ij}, T_{ij}, \ln p(O_2)_i\}$	10	-	$p = 1.3 \cdot 10^{-4}$	TGA	89BRY/GAL
ZBA	$\{z_{ij}, T_{ij}, \ln p(O_2)_i\}$	4	-	$p = 1.8 \cdot 10^{-5}$	TGA	89BRY/GAL

Table 2. Continued

Code	Set of values	N_i	Inc.	v_i	Method	Reference
ZF0	$\{z_{ij}, T_{ij}, \ln p(O_2)_i\}$	12	-	p = 1	TGA	90FUE/IDE
ZF1	$\{z_{ij}, T_{ij}, \ln p(O_2)_i\}$	12	-	p = 0.4	TGA	90FUE/IDE
ZF2	$\{z_{ij}, T_{ij}, \ln p(O_2)_i\}$	11	-	p = 0.1	TGA	90FUE/IDE
ZF3	$\{z_{ij}, T_{ij}, \ln p(O_2)_i\}$	10	-	p = 0.05	TGA	90FUE/IDE
ZF4	$\{z_{ij}, T_{ij}, \ln p(O_2)_i\}$	9	-	p = 0.007	TGA	90FUE/IDE
ZK0	$\{z_{ij}, T_{ij}, \ln p(O_2)_i\}$	12	-	p = 1	TGA	94KIM/GAS
ZK2	$\{z_{ij}, T_{ij}, \ln p(O_2)_i\}$	12	-	p = 0.1	TGA	94KIM/GAS
ZK4	$\{z_{ij}, T_{ij}, \ln p(O_2)_i\}$	11	-	p = 0.01	TGA	94KIM/GAS
ZK6	$\{z_{ij}, T_{ij}, \ln p(O_2)_i\}$	10	-	p = 0.001	TGA	94KIM/GAS
ZK8	$\{z_{ij}, T_{ij}, \ln p(O_2)_i\}$	8	-	$p = 1 \cdot 10^{-4}$	TGA	94KIM/GAS
ZKA	$\{z_{ij}, T_{ij}, \ln p(O_2)_i\}$	8	-	$p = 1 \cdot 10^{-5}$	TGA	94KIM/GAS
ZKC	$\{z_{ij}, T_{ij}, \ln p(O_2)_i\}$	3	-	$p = 1 \cdot 10^{-6}$	TGA	94KIM/GAS
ZL0	$\{z_{ij}, T_{ij}, \ln p(O_2)_i\}$	25	+	p = 1	TGA	89LIN/HUN
ZL2	$\{z_{ij}, T_{ij}, \ln p(O_2)_i\}$	12	+	p = 0.1	TGA	89LIN/HUN
ZL4	$\{z_{ij}, T_{ij}, \ln p(O_2)_i\}$	11	+	p = 0.01	TGA	89LIN/HUN
ZL6	$\{z_{ij}, T_{ij}, \ln p(O_2)_i\}$	9	+	p = 0.001	TGA	89LIN/HUN
ZL8	$\{z_{ij}, T_{ij}, \ln p(O_2)_i\}$	6	+	$p = 1 \cdot 10^{-4}$	TGA	89LIN/HUN
ZLA	$\{z_{ij}, T_{ij}, \ln p(O_2)_i\}$	2	+	$p = 1 \cdot 10^{-5}$	TGA	89LIN/HUN
ZV0	$\{z_{ij}, T_{ij}, \ln p(O_2)_i\}$	7	+	p = 0.89	analysis	89VER/BRU
ZC0	$\{z_{ij}, T_{ij}, \ln p(O_2)_i\}$	16	+	p = 1	TGA	92CON/KAR
ZC0a	$\{z_{ij}, T_{ij}, \ln p(O_2)_i\}$	13	+	p = 1	TGA	92CON/KAR
ZC2	$\{z_{ij}, T_{ij}, \ln p(O_2)_i\}$	10	+	p = 0.09	TGA	92CON/KAR
ZC4	$\{z_{ij}, T_{ij}, \ln p(O_2)_i\}$	7	+	p = 0.01	TGA	92CON/KAR
ZC6	$\{z_{ij}, T_{ij}, \ln p(O_2)_i\}$	6	+	p = 0.0017	TGA	92CON/KAR
ZCK	$\{z_{ij}, T_{ij}, \ln p(O_2)_i\}$	13	+	p = 4	TGA	92CON/KAR
ZCL	$\{z_{ij}, T_{ij}, \ln p(O_2)_i\}$	11	+	p = 11	TGA	92CON/KAR
ZCM	$\{z_{ij}, T_{ij}, \ln p(O_2)_i\}$	9	+	p = 50	TGA	92CON/KAR
Os9	$\{\ln p(O_2)_{ij}, z_{ij}, T_i\}$	22	-	T = 838 K	VA	87SAL/KOE
OsB	$\{\ln p(O_2)_{ij}, z_{ij}, T_i\}$	23	-	T = 884 K	VA	87SAL/KOE
OsD	$\{\ln p(O_2)_{ij}, z_{ij}, T_i\}$	21	-	T = 926 K	VA	87SAL/KOE
OsG	$\{\ln p(O_2)_{ij}, z_{ij}, T_i\}$	18	-	T = 990 K	VA	87SAL/KOE
OsJ	$\{\ln p(O_2)_{ij}, z_{ij}, T_i\}$	11	-	T = 1081 K	VA	87SAL/KOE
OBD	$\{\ln p(O_2)_{ij}, z_{ij}, T_i\}$	5	-	T = 913 K	emf	89BOR/NOL
OBG	$\{\ln p(O_2)_{ij}, z_{ij}, T_i\}$	4	-	T = 993 K	emf	89BOR/NOL
OBH	$\{\ln p(O_2)_{ij}, z_{ij}, T_i\}$	4	-	T = 1023 K	emf	89BOR/NOL
OK1	$\{\ln p(O_2)_{ij}, z_{ij}, T_i\}$	4	-	T = 623 K	TGA	87KIS/SHI
OK3	$\{\ln p(O_2)_{ij}, z_{ij}, T_i\}$	4	-	T = 673 K	TGA	87KIS/SHI
OK5	$\{\ln p(O_2)_{ij}, z_{ij}, T_i\}$	7	-	T = 723 K	TGA	87KIS/SHI
OK7	$\{\ln p(O_2)_{ij}, z_{ij}, T_i\}$	11	-	T = 773 K	TGA	87KIS/SHI
OK9	$\{\ln p(O_2)_{ij}, z_{ij}, T_i\}$	12	-	T = 823 K	TGA	87KIS/SHI
OKB	$\{\ln p(O_2)_{ij}, z_{ij}, T_i\}$	11	-	T = 873 K	TGA	87KIS/SHI
OKD	$\{\ln p(O_2)_{ij}, z_{ij}, T_i\}$	12	-	T = 923 K	TGA	87KIS/SHI
OKF	$\{\ln p(O_2)_{ij}, z_{ij}, T_i\}$	10	-	T = 973 K	TGA	87KIS/SHI
OKH	$\{\ln p(O_2)_{ij}, z_{ij}, T_i\}$	10	-	T = 1023 K	TGA	87KIS/SHI
OKJ	$\{\ln p(O_2)_{ij}, z_{ij}, T_i\}$	9	-	T = 1073 K	TGA	87KIS/SHI
OKL	$\{\ln p(O_2)_{ij}, z_{ij}, T_i\}$	9	-	T = 1123 K	TGA	87KIS/SHI
OKN	$\{\ln p(O_2)_{ij}, z_{ij}, T_i\}$	7	-	T = 1173 K	TGA	87KIS/SHI
OKQ	$\{\ln p(O_2)_{ij}, z_{ij}, T_i\}$	7	-	T = 1223 K	TGA	87KIS/SHI
OKS	$\{\ln p(O_2)_{ij}, z_{ij}, T_i\}$	4	-	T = 1273 K	TGA	87KIS/SHI

Table 2. Continued

Code	Set of values	N_i	Inc.	v_i	Method	Reference
OT7	$\{\ln p(O_2)_{ij}, z_{ij}, T_i\}$	5	-	T = 773 K	TGA	88TOU/MAR
OTB	$\{\ln p(O_2)_{ij}, z_{ij}, T_i\}$	4	-	T = 873 K	TGA	88TOU/MAR
OTJ	$\{\ln p(O_2)_{ij}, z_{ij}, T_i\}$	3	-	T = 1073 K	TGA	88TOU/MAR
OS7	$\{\ln p(O_2)_{ij}, z_{ij}, T_i\}$	10	-	T = 776 K	TGA	88SPE/SPA
OSB	$\{\ln p(O_2)_{ij}, z_{ij}, T_i\}$	10	-	T = 861 K	TGA	88SPE/SPA
OSD	$\{\ln p(O_2)_{ij}, z_{ij}, T_i\}$	10	-	T = 938 K	TGA	88SPE/SPA
OSH	$\{\ln p(O_2)_{ij}, z_{ij}, T_i\}$	10	-	T = 1012 K	TGA	88SPE/SPA
OSJ	$\{\ln p(O_2)_{ij}, z_{ij}, T_i\}$	10	-	T = 1070 K	TGA	88SPE/SPA
OSM	$\{\ln p(O_2)_{ij}, z_{ij}, T_i\}$	10	-	T = 1148 K	TGA	88SPE/SPA
OM3	$\{\ln p(O_2)_{ij}, z_{ij}, T_i\}$	19	-	T = 673 K	VA	89MEU/NAE
OM4	$\{\ln p(O_2)_{ij}, z_{ij}, T_i\}$	20	-	T = 698 K	VA	89MEU/NAE
OM5	$\{\ln p(O_2)_{ij}, z_{ij}, T_i\}$	22	-	T = 723 K	VA	89MEU/NAE
OM6	$\{\ln p(O_2)_{ij}, z_{ij}, T_i\}$	20	-	T = 748 K	VA	89MEU/NAE
OM7	$\{\ln p(O_2)_{ij}, z_{ij}, T_i\}$	26	-	T = 773 K	VA	89MEU/NAE
OM8	$\{\ln p(O_2)_{ij}, z_{ij}, T_i\}$	25	-	T = 798 K	VA	89MEU/NAE
OM9	$\{\ln p(O_2)_{ij}, z_{ij}, T_i\}$	26	-	T = 823 K	VA	89MEU/NAE
OMA	$\{\ln p(O_2)_{ij}, z_{ij}, T_i\}$	28	-	T = 848 K	VA	89MEU/NAE
OMB	$\{\ln p(O_2)_{ij}, z_{ij}, T_i\}$	28	-	T = 873 K	VA	89MEU/NAE
OMC	$\{\ln p(O_2)_{ij}, z_{ij}, T_i\}$	30	-	T = 898 K	VA	89MEU/NAE
OMD	$\{\ln p(O_2)_{ij}, z_{ij}, T_i\}$	30	-	T = 923 K	VA	89MEU/NAE
OME	$\{\ln p(O_2)_{ij}, z_{ij}, T_i\}$	31	-	T = 948 K	VA	89MEU/NAE
OMF	$\{\ln p(O_2)_{ij}, z_{ij}, T_i\}$	32	-	T = 973 K	VA	89MEU/NAE
OMG	$\{\ln p(O_2)_{ij}, z_{ij}, T_i\}$	32	-	T = 998 K	VA	89MEU/NAE
OMH	$\{\ln p(O_2)_{ij}, z_{ij}, T_i\}$	30	-	T = 1023 K	VA	89MEU/NAE
Ot3	$\{\ln p(O_2)_{ij}, z_{ij}, T_i\}$	26	-	T = 673 K	emf	89TET/TAN
Ot4	$\{\ln p(O_2)_{ij}, z_{ij}, T_i\}$	27	-	T = 698 K	emf	89TET/TAN
Ot5	$\{\ln p(O_2)_{ij}, z_{ij}, T_i\}$	27	-	T = 723 K	emf	89TET/TAN
Ot6	$\{\ln p(O_2)_{ij}, z_{ij}, T_i\}$	28	-	T = 748 K	emf	89TET/TAN
Ot7	$\{\ln p(O_2)_{ij}, z_{ij}, T_i\}$	29	-	T = 773 K	emf	89TET/TAN
Ot9	$\{\ln p(O_2)_{ij}, z_{ij}, T_i\}$	28	-	T = 823 K	emf	89TET/TAN
OtB	$\{\ln p(O_2)_{ij}, z_{ij}, T_i\}$	24	-	T = 873 K	emf	89TET/TAN
OGB	$\{\ln p(O_2)_{ij}, z_{ij}, T_i\}$	38	+	T = 873 K	TGA	89GER/PIC
Oc5	$\{\ln p(O_2)_{ij}, z_{ij}, T_i\}$	28	+	T = 723 K	VA	91SCH/HAR
Oc6	$\{\ln p(O_2)_{ij}, z_{ij}, T_i\}$	36	+	T = 748 K	VA	91SCH/HAR
Oc7	$\{\ln p(O_2)_{ij}, z_{ij}, T_i\}$	33	+	T = 773 K	VA	91SCH/HAR
Oc9	$\{\ln p(O_2)_{ij}, z_{ij}, T_i\}$	32	+	T = 823 K	VA	91SCH/HAR
OcB	$\{\ln p(O_2)_{ij}, z_{ij}, T_i\}$	30	+	T = 873 K	VA	91SCH/HAR
OcD	$\{\ln p(O_2)_{ij}, z_{ij}, T_i\}$	28	+	T = 923 K	VA	91SCH/HAR
Om7	$\{\ln p(O_2)_{ij}, z_{ij}, T_i\}$	19	+	T = 773 K	emf	92MAT/JAC
OmB	$\{\ln p(O_2)_{ij}, z_{ij}, T_i\}$	18	+	T = 873 K	emf	92MAT/JAC
OmF	$\{\ln p(O_2)_{ij}, z_{ij}, T_i\}$	12	+	T = 973 K	emf	92MAT/JAC
OmJ	$\{\ln p(O_2)_{ij}, z_{ij}, T_i\}$	8	+	T = 1073 K	emf	92MAT/JAC
OmN	$\{\ln p(O_2)_{ij}, z_{ij}, T_i\}$	6	+	T = 1173 K	emf	92MAT/JAC
OmQ	$\{\ln p(O_2)_{ij}, z_{ij}, T_i\}$	6	+	T = 1273 K	emf	92MAT/JAC

Table 2. Continued

Code	Set of values	N_i	Inc.	v_i	Method	Reference
N1	$\{\ln p(O_2)_{ij}, T_{ij}, z_i\}$	55	-	z = 0.978	VA	89VER/BRU
N2	$\{\ln p(O_2)_{ij}, T_{ij}, z_i\}$	55	+	z = 0.922	VA	89VER/BRU
N3	$\{\ln p(O_2)_{ij}, T_{ij}, z_i\}$	44	+	z = 0.801	VA	89VER/BRU
N4	$\{\ln p(O_2)_{ij}, T_{ij}, z_i\}$	77	+	z = 0.632	VA	89VER/BRU
N5	$\{\ln p(O_2)_{ij}, T_{ij}, z_i\}$	66	+	z = 0.508	VA	89VER/BRU
N6	$\{\ln p(O_2)_{ij}, T_{ij}, z_i\}$	55	+	z = 0.404	VA	89VER/BRU
N7	$\{\ln p(O_2)_{ij}, T_{ij}, z_i\}$	22	+	z = 0.285	VA	89VER/BRU
VT1	$\{\ln p(O_2)_{ij}, T_{ij}, V_i\}^{d}$	86	-	n/a	VA	94TAR/GUS
VT2	$\{\ln p(O_2)_{ij}, T_{ij}, V_i\}^{d}$	41	-	n/a	VA	94TAR/GUS
VT3	$\{\ln p(O_2)_{ij}, T_{ij}, V_i\}^{d}$	39	-	n/a	VA	94TAR/GUS
VT4	$\{\ln p(O_2)_{ij}, T_{ij}, V_i\}^{d}$	28	-	n/a	VA	94TAR/GUS
VT5	$\{\ln p(O_2)_{ij}, T_{ij}, V_i\}^{d}$	41	-	n/a	VA	94TAR/GUS
VT6	$\{\ln p(O_2)_{ij}, T_{ij}, V_i\}^{d}$	51	-	n/a	VA	94TAR/GUS
VT7	$\{\ln p(O_2)_{ij}, T_{ij}, V_i\}^{d}$	35	-	n/a	VA	94TAR/GUS
VT8	$\{\ln p(O_2)_{ij}, T_{ij}, V_i\}^{d}$	50	-	n/a	VA	94TAR/GUS
VT9	$\{\ln p(O_2)_{ij}, T_{ij}, V_i\}^{d}$	29	-	n/a	VA	94TAR/GUS
VTA	$\{\ln p(O_2)_{ij}, T_{ij}, V_i\}^{d}$	30	-	n/a	VA	94TAR/GUS
VTB	$\{\ln p(O_2)_{ij}, T_{ij}, V_i\}^{d}$	31	-	n/a	VA	94TAR/GUS
VTC	$\{\ln p(O_2)_{ij}, T_{ij}, V_i\}^{d}$	40	-	n/a	VA	94TAR/GUS
VTD	$\{\ln p(O_2)_{ij}, T_{ij}, V_i\}^{d}$	47	-	n/a	VA	94TAR/GUS
VTE	$\{\ln p(O_2)_{ij}, T_{ij}, V_i\}^{d}$	43	-	n/a	VA	94TAR/GUS
VTF	$\{\ln p(O_2)_{ij}, T_{ij}, V_i\}^{d}$	43	-	n/a	VA	94TAR/GUS
VTG	$\{\ln p(O_2)_{ij}, T_{ij}, V_i\}^{d}$	47	-	n/a	VA	94TAR/GUS
PG	$\{\Delta_{ox}H'_{O,ij}, z_{ij}, T_i\}$	19	-	T = 873 K	calorimetry	89GER/PIC
PP1	$\{\Delta H_{ij}, z'_{ij}, T'_i\}^{e}$	10	+	n/a	calorimetry	89PAR/NAV
PP2	$\{\Delta H_{ij}, z'_{ij}, T'_i\}^{e}$	14	+	n/a	calorimetry	89PAR/NAV
PP3	$\{\Delta H_{ij}, z'_{ij}, T'_i\}^{e}$	3	+	n/a	calorimetry	89PAR/NAV
S	$\{S_{ij}, z_{ij}, T_i\}$	6	+	T = 298 K	AC	f
CG7	$\{C_{pz,ij}, T_{ij}, z_i\}$	7	+	z = 0.70	AC	88GAV/GOR
CG9	$\{C_{pz,ij}, T_{ij}, z_i\}$	7	+	z = 0.85	AC	88GAV/GOR
CJ9	$\{C_{pz,ij}, T_{ij}, z_i\}$	5	+	z = 0.9	AC	89JUN/ECK
CS9	$\{C_{pz,ij}, T_{ij}, z_i\}$	9	+	z = 0.9	AC	90SHA/WES
CAA	$\{C_{pz,ij}, T_{ij}, z_i\}$	7	+	z = 0.96	AC	91ATA/HON
CsA	$\{C_{pz,ij}, T_{ij}, z_i\}$	2	+	z = 1.0	AC	88SHE/CHU
CM4	$\{C_{pz,ij}, T_{ij}, z_i\}$	9	-	z = 0.4	DSC	90MAT/FUJ
CM7	$\{C_{pz,ij}, T_{ij}, z_i\}$	11	-	z = 0.65	DSC	90MAT/FUJ
CM8	$\{C_{pz,ij}, T_{ij}, z_i\}$	10	-	z = 0.82	DSC	90MAT/FUJ
Ca5	$\{C_{pz,ij}, T_{ij}, z_i\}$	21	-	z = 0.5	DSC	91SHA/OZE
Ca9	$\{C_{pz,ij}, T_{ij}, z_i\}$	20	-	z = 0.85	DSC	91SHA/OZE
HG	$\{\Delta_{ox}H_{ij}, z_{ij}, T_i\}$		-	T = 298 K	calorimetry	89GRU/PIV
Hg	$\{\Delta_{ox}H_{ij}, z_{ij}, T_i\}$		-	T = 298 K	calorimetry	91GAR/RAI
HC	$\{\Delta_{ox}H_{ij}, z_{ij}, T_i\}$		-	T = 298 K	calorimetry	92CHO/KAN
HI	$\{\Delta_{ox}H_{ij}, z_{ij}, T_i\}$		-	T = 298 K	calorimetry	92IDE/TAK
HP	$\{\Delta_{ox}H_{ij}, z_{ij}, T_i\}$		-	T = 298 K	calorimetry	93PRI/ZIN

Table 2. Continued

Code	Set of values	N_i	Inc.	v_i	Method	Reference
HM	$\{\Delta_{ox}H_{ij}, z_{ij}, T_i\}$	4	+	$T = 298$ K	calorimetry	88MOR/SON
Hm	$\{\Delta_{ox}H_{ij}, z_{ij}, T_i\}$	2	+	$T = 298$ K	calorimetry	95MON/POP
Ha	$\{\Delta_{ox}H_{ij}, z_{ij}, T_i\}$	5	+	$T = 298$ K	calorimetry	93MAT/POP
HZ	$\{\Delta_{ox}H_{ij}, z_{ij}, T_i\}$	7	+	$T = 298$ K	calorimetry	92ZHO/NAV
HH	$\{\Delta_{ox}H_{ij}, z_{ij}, T_i\}$		-	$T = 298$ K	calorimetry	95HEN/ZHE
GA	$\{\Delta_{ox}G_{ij}, T_{ij}, \ln p(O_2)_i\}$		-	$p = 1$	emf	90AZA/SRE
GF	$\{\Delta_{ox}G_{ij}, T_{ij}, \ln p(O_2)_i\}$		-	$p = 0.21$	emf	90FAN/JI
GS	$\{\Delta_{ox}G_{ij}, T_{ij}, \ln p(O_2)_i\}$	26	+	$p = 1$	emf	91SKO/PAS

[a] Plus means that the experiment is included into the final assessment, minus means that it is not.

[b] p in this column means dimentionless quantity p/p^o, where $p^o = 101325$ Pa.

[c] XRD - X-ray diffraction, TGA - thermal gravimetry analysis, ND - neutron diffraction, VA - volumetric analysis, emf - electromotive force, AC - adiabatic calorimetry, DSC - differential scanning calorimetry.

[d] The experimental point looks like $\{\ln p(O_2)_{ij}, T_{ij}, V_i, z_i^o, m_i^o\}$

[e] The experimental point looks like $\{\Delta H_{ij}, z'_{ij}, T'_i, z''_i, T''_i\}$

[f] The references are 88GAV/GOR, 89JUN/ECK, 90SHA/WES, 91ATA/HON, 88SHE/CHU.

Table 3. Grouping the experiments

Quantity	Group	Codes of the experiments	Inc.[a]
Temperature of T-O phase transition	T_O	TB1, TE, TF, TK, TT, TY, To, Tp, Tu, TW, TB2	+[b]
Temperature of T-O phase transition	T_z	TM1, TM2	-
Oxygen occupancies	X	XJ0, XJ1, XJ3, XI1	+
Index z	Z_b	ZJ0, ZJ1, ZJ3, ZI1	-
Index z	Z_g	Zt0, Zt1, Zt3, Zt4, Zt6, ZS0, ZS1, ZT0, ZT1, ZY0, ZY0a, ZY1, ZY1a, ZY3, ZY4, ZY5, ZY6, ZY7, ZB8, ZBA, ZF0, ZF1, ZF2, ZF3, ZF4, ZK0, ZK2, ZK4, ZK6, ZK8, ZKA, ZKC	-
Index z	Z	ZL0, ZL2, ZL4, ZL6, ZL8, ZLA, ZV0, ZC0, ZC0a, ZC2, ZC4, ZC6, ZCK, ZCL, ZCM	+
Oxygen partial pressure (T = const)	O_b	Os9, OsB, OsD, OsG, OsJ, OBD, OBG, OBH, OK1, OK3, OK5, OK7	-
Oxygen partial pressure (T = const)	O_g	OK9, OKB, OKD, OKF, OKH, OKJ, OKL, OKN, OKQ, OKS, OT7, OTB, OTJ, OS7, OSB, OSD, OSH, OSJ, OSM, OM3, OM4, OM5, OM6, OM7, OM8, OM9, OMA, OMB, OMC, OMD, OME, OMF, OMG, OMH, Ot3, Ot4, Ot5, Ot6, Ot7, Ot9, OtB	-
Oxygen partial pressure (T = const)	O	OGB, Oc5, Oc6, Oc7, Oc9, OcB, OcD, Om7, OmB, OmF, OmJ, OmN, OmQ	+
Oxygen partial pressure (z = const)	N	N2, N3, N4, N5, N6, N7	+[c]
Oxygen partial pressure (V = const)	V	VT1, VT2, VT3, VT4, VT5, VT6, VT7, VT8, VT9, VTA, VTB, VTC, VTD, VTE, VTF, VTG	-
Partial enthalpy	P_b	PG	-
Drop enthalpy	P	PP1, PP2, PP3	+
Entropy	S	S	+
Heat capacity	C	CG7, CG9, CJ9, CS9, CAA, CsA	+
Heat capacity	C_h	CM4, CM7, CM8, Ca5, Ca9	-
Enthalpy	H_b	HG, Hg, HC, HI, HP	-.
Enthalpy	H	HM, Hm, Ha, HZ, HH	+
Gibbs energy	G_b	GA, GF	-
Gibbs energy	G	GS	+

[a] Plus means that the group is included into the final assessment, minus means that it is not. Explanations are in Section 4.2.

[b] Ts was excluded because it was assumed to be the outlier.

[c] N1 was excluded because it was assumed to be the outlier.

Table 4. The variance components obtained

group	$\sqrt{\sigma_{r,i}^2}$	$\sqrt{\gamma_a}$	$\sqrt{\gamma_b}$
T_O	11.4 K	2.61	7.19
X	0.0388	2.61	7.19
Z	0.00743	2.61	7.19
O	0.106	2.61	7.19
N	0.156	2.61	7.19
P	4.54 kJ·mol^{-1}	2.61	7.19
S	2.51 J·K^{-1}mol^{-1}	2.61	7.19
C	0.813 J·K^{-1}mol^{-1}	2.61	7.19
H	5.01 kJ·mol^{-1}	2.61	7.19
G	1.00 kJ·mol^{-1}	2.61	7.19

Table 5. The parameters obtained in solution ML[a]

	A	B	C	D
g_1	-3564 ± 541	-4.918 ± 0.490	0	0
g_2	-10360 ± 160	45.99 ± 4.59	-4.051 ± 0.518	-252.3 ± 33.7
a_1	2000 ± 165	-1.544 ± 0.204	0	0
a_2	-2590 ± 224	4.044 ± 0.279	0	0
b_1	652.1 ± 164	3.921 ± 0.193	0	0

[a] See Eq. (2) and (21). The parameters lead to the Gibbs energy normalized by the gas constant, *G/R*.

Table 6. Thermodynamic properties of the YBa$_2$Cu$_3$O$_{6+z}$ phase

T/K	z	x	C_{pz}^{o} J·mol^{-1}K^{-1}	S^{o} J·mol^{-1}K^{-1}	$H^{o} - H^{o}_{298}$ kJ·mol^{-1}	$\Delta_{ox}H^{o}$ kJ·mol^{-1}	$\ln \frac{p(O_2)}{p^{o}}$
298.15	0.00	0.00	265.64	311.10	0.00	-29.63	-∞
300.00	0.00	0.00	266.14	312.74	0.49	-29.63	-∞
400.00	0.00	0.00	287.66	392.48	28.26	-29.63	-∞
500.00	0.00	0.00	302.12	458.32	57.79	-29.63	-∞
600.00	0.00	0.00	312.62	514.38	88.56	-29.63	-∞
700.00	0.00	0.00	320.66	563.20	120.24	-29.63	-∞
800.00	0.00	0.00	327.08	606.45	152.63	-29.63	-∞
900.00	0.00	0.00	332.34	645.29	185.61	-29.63	-∞
1000.00	0.00	0.00	336.77	680.54	219.07	-29.63	-∞
1100.00	0.00	0.00	340.55	712.82	252.94	-29.63	-∞
1200.00	0.00	0.00	343.84	742.59	287.17	-29.63	-∞
298.15	0.25	0.00	270.14	320.85	0.00	-53.01	-54.04
300.00	0.25	0.00	270.66	322.52	0.50	-53.01	-53.60
400.00	0.25	0.00	293.29	403.72	28.78	-52.87	-35.75
500.00	0.25	0.00	308.57	470.90	58.92	-52.64	-25.13
600.00	0.25	0.00	319.70	528.20	90.36	-52.36	-18.14
700.00	0.25	0.00	328.25	578.15	122.77	-52.04	-13.21
800.00	0.25	0.00	335.07	622.44	155.95	-51.67	-9.57
900.00	0.25	0.00	340.68	662.24	189.75	-51.28	-6.79
1000.00	0.25	0.00	345.39	698.38	224.06	-50.86	-4.61
1100.00	0.25	0.00	349.43	731.50	258.80	-50.43	-2.87
1200.00	0.25	0.00	352.93	762.06	293.92	-49.97	-1.45
298.15	0.50	0.16	275.60	326.08	0.00	-75.07	-50.21
300.00	0.50	0.16	276.14	327.78	0.51	-75.07	-49.77
400.00	0.50	0.09	299.75	410.70	29.30	-74.70	-31.94
500.00	0.50	0.00	315.03	479.35	60.04	-74.20	-21.40
600.00	0.50	0.00	326.79	537.88	92.16	-73.64	-14.54
700.00	0.50	0.00	335.84	588.96	125.31	-72.98	-9.72
800.00	0.50	0.00	343.07	634.29	159.27	-72.26	-6.16
900.00	0.50	0.00	349.02	675.05	193.88	-71.47	-3.44
1000.00	0.50	0.00	354.02	712.09	229.04	-70.64	-1.31
1100.00	0.50	0.00	358.31	746.04	264.66	-69.76	0.40
1200.00	0.50	0.00	362.03	777.38	300.68	-68.85	1.79

Table 6. Continued

T/K	z	x	C_{pz}^o $J \cdot mol^{-1} K^{-1}$	S^o $J \cdot mol^{-1} K^{-1}$	$H^o - H^o_{298}$ $kJ \cdot mol^{-1}$	$\Delta_{ox}H^o$ $kJ \cdot mol^{-1}$	$\ln \frac{p(O_2)}{p^o}$
298.15	0.75	0.34	280.05	326.98	0.00	-98.03	-50.69
300.00	0.75	0.34	280.62	328.72	0.52	-98.02	-50.21
400.00	0.75	0.31	305.39	413.09	29.82	-97.51	-31.06
500.00	0.75	0.29	322.21	483.15	61.16	-96.76	-19.66
600.00	0.75	0.26	334.50	543.04	93.96	-95.85	-12.15
700.00	0.75	0.24	343.96	595.34	127.85	-94.81	-6.86
800.00	0.75	0.22	351.52	641.78	162.58	-93.67	-2.95
900.00	0.75	0.20	357.75	683.55	198.01	-92.45	0.04
1000.00	0.75	0.19	362.99	721.53	234.02	-91.16	2.38
1100.00	0.75	0.17	367.48	756.34	270.52	-89.82	4.27
1200.00	0.75	0.15	371.39	788.49	307.44	-88.43	5.80
298.15	1.00	0.43	285.09	319.68	0.00	-123.50	$+\infty$
300.00	1.00	0.43	285.68	321.44	0.53	-123.49	$+\infty$
400.00	1.00	0.40	311.37	407.41	30.33	-122.80	$+\infty$
500.00	1.00	0.38	328.91	478.88	62.29	-121.80	$+\infty$
600.00	1.00	0.36	341.76	540.04	95.76	-120.58	$+\infty$
700.00	1.00	0.34	351.68	593.50	130.38	-119.20	$+\infty$
800.00	1.00	0.32	359.62	640.99	165.90	-117.69	$+\infty$
900.00	1.00	0.30	366.17	683.74	202.15	-116.07	$+\infty$
1000.00	1.00	0.29	371.68	722.61	239.00	-114.36	$+\infty$
1100.00	1.00	0.28	376.41	758.27	276.38	-112.57	$+\infty$
1200.00	1.00	0.27	380.53	791.20	314.20	-110.72	$+\infty$

Table 7. The correlation matrix for the parameters obtained in solution ML

	$g_{1,A}$	$g_{1,B}$	$g_{2,A}$	$g_{2,B}$	$g_{2,C}$	$g_{2,D}$
$g_{1,A}$	1	-	-	-	-	-
$g_{1,B}$	-0.8456	1	-	-	-	-
$g_{2,A}$	-0.1218	0.1345	1	-	-	-
$g_{2,B}$	0.1600	-0.1655	0.2049	1	-	-
$g_{2,C}$	-0.1588	0.1640	-0.2007	-0.9992	1	-
$g_{2,D}$	-0.1353	0.1394	-0.3648	-0.9787	0.9727	1
$a_{1,A}$	-0.05636	0.06241	-0.09119	-0.2819	0.2870	0.2644
$a_{1,B}$	0.03600	-0.04097	0.1732	0.2677	-0.2758	-0.2549
$a_{2,A}$	-0.04552	0.05858	0.2790	0.04880	-0.06001	-0.05707
$a_{2,B}$	0.04405	-0.05768	-0.2795	-0.04931	0.06060	0.05815
$b_{1,A}$	-0.04051	0.04131	0.01065	-0.3108	0.3184	0.2680
$b_{1,B}$	0.04406	-0.04575	-0.03082	0.3079	-0.3148	-0.2641

	$a_{1,A}$	$a_{1,B}$	$a_{2,A}$	$a_{2,B}$	$b_{1,A}$	$b_{1,B}$
$a_{1,A}$	1	-	-	-	-	-
$a_{1,B}$	-0.9832	1	-	-	-	-
$a_{2,A}$	-0.6399	0.6645	1	-	-	-
$a_{2,B}$	0.6637	-0.6948	-0.9926	1	-	-
$b_{1,A}$	0.002190	0.01899	0.03187	-0.05097	1	-
$b_{1,B}$	0.01712	-0.04418	-0.06832	0.08911	-0.9914	1
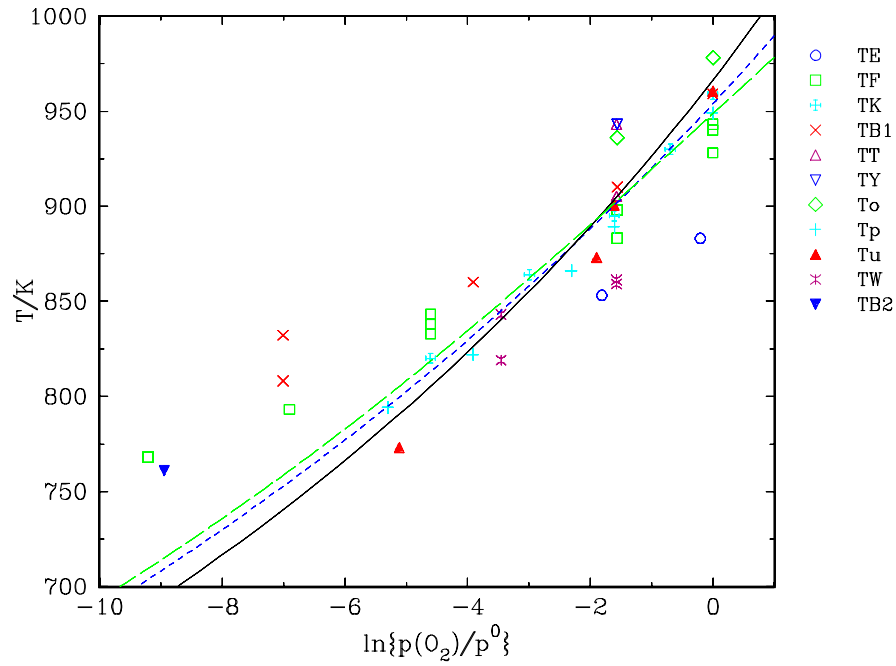
Fig. 1. The temperatures of the phase transition as a function of the oxygen partial pressure. The solid line is solution ML, the long dashed line is solution WLS, the short dashed line is the solution by 93DEG/VOR.
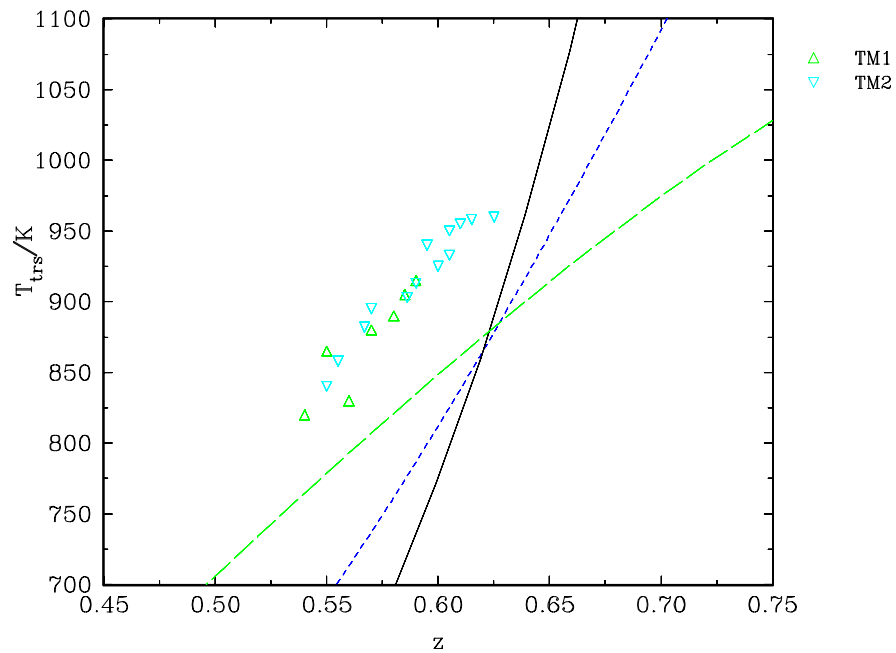
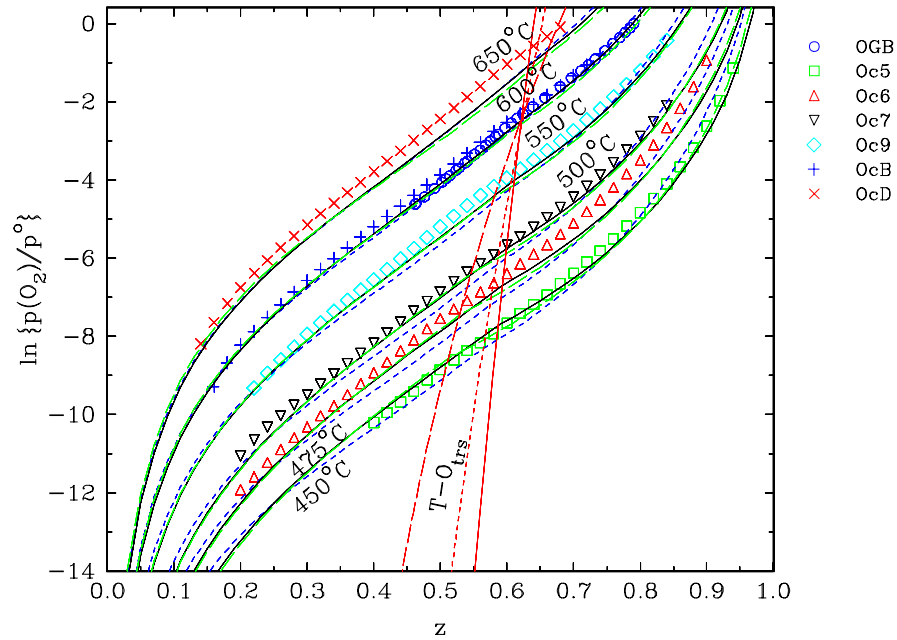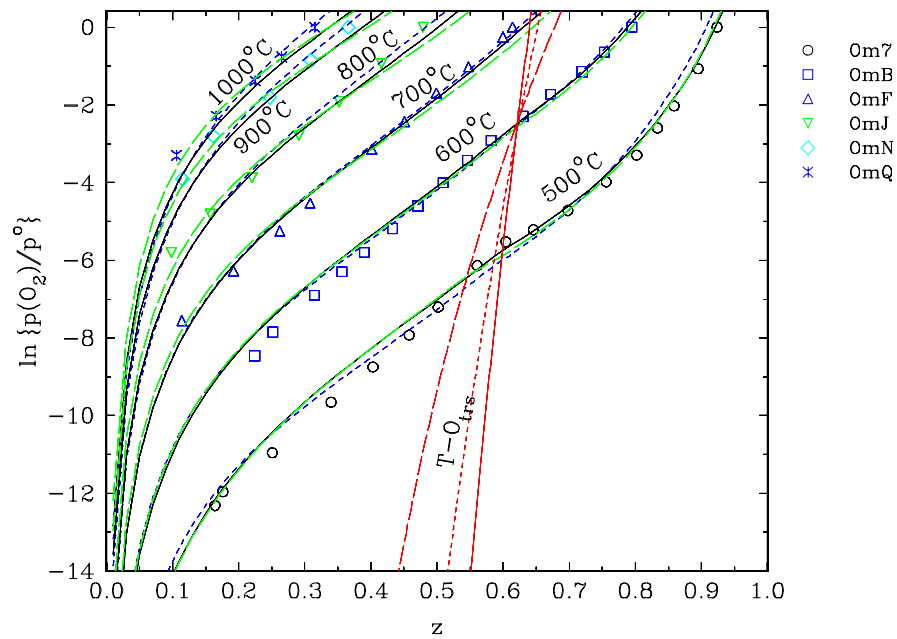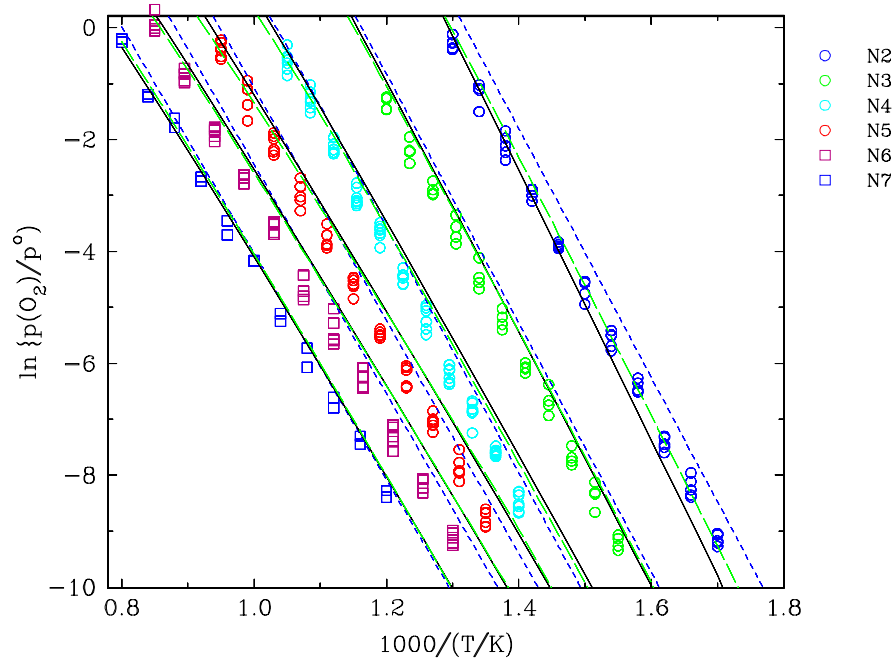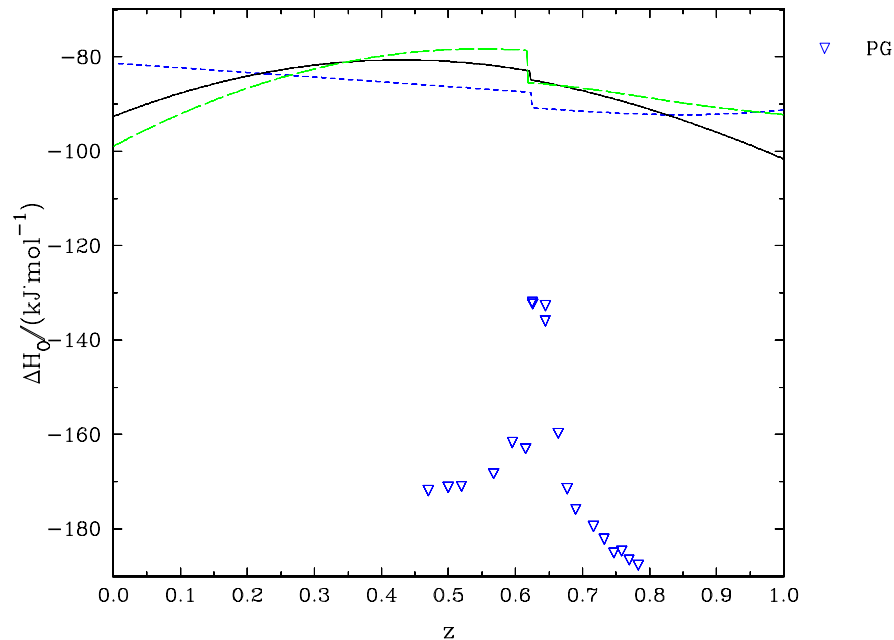**Fig. 2. The temperatures of the phase transition as a function of index *z*. The solid line is solution ML, the long dashed line is solution WLS, the short dashed line is the solution by 93DEG/VOR.**
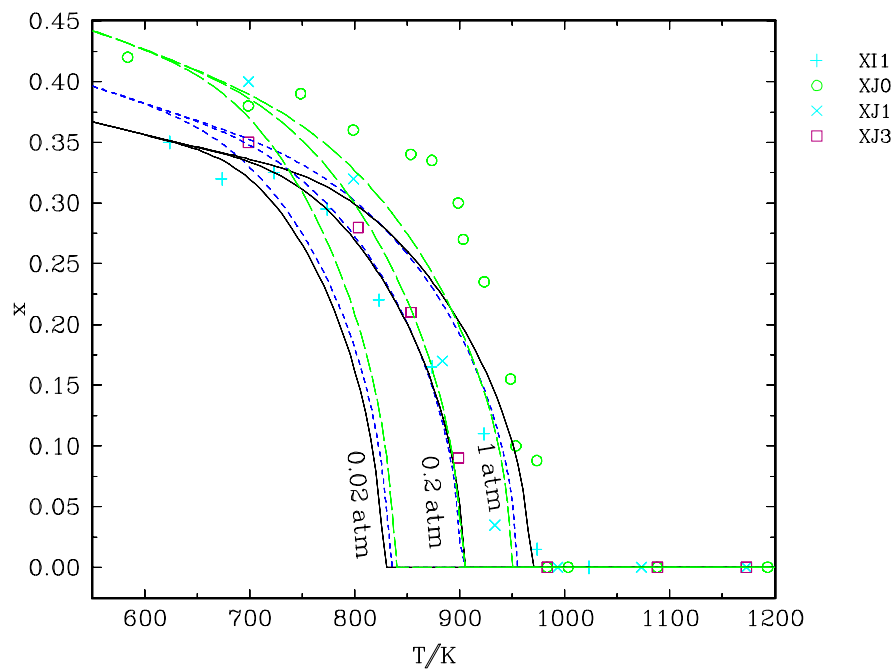
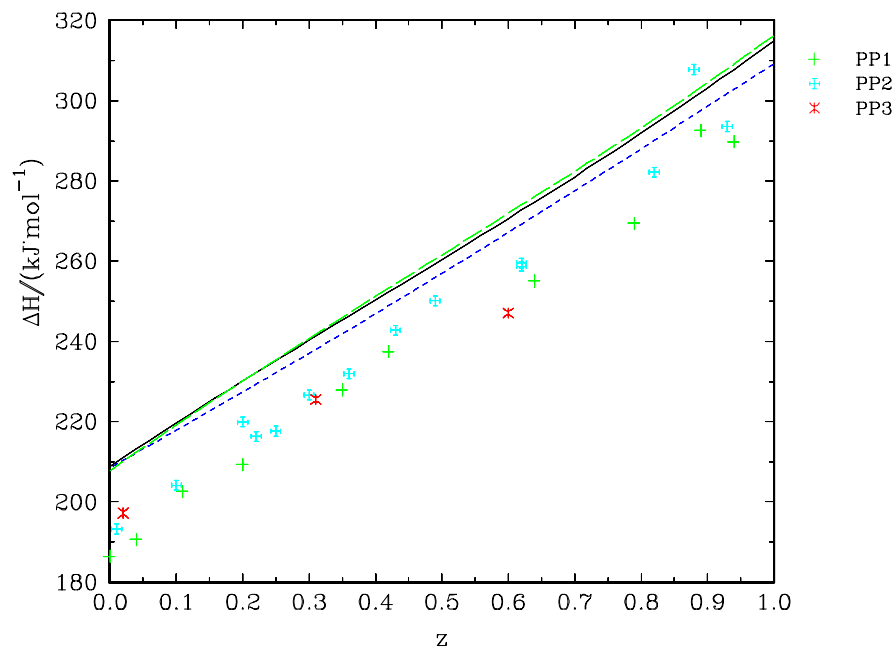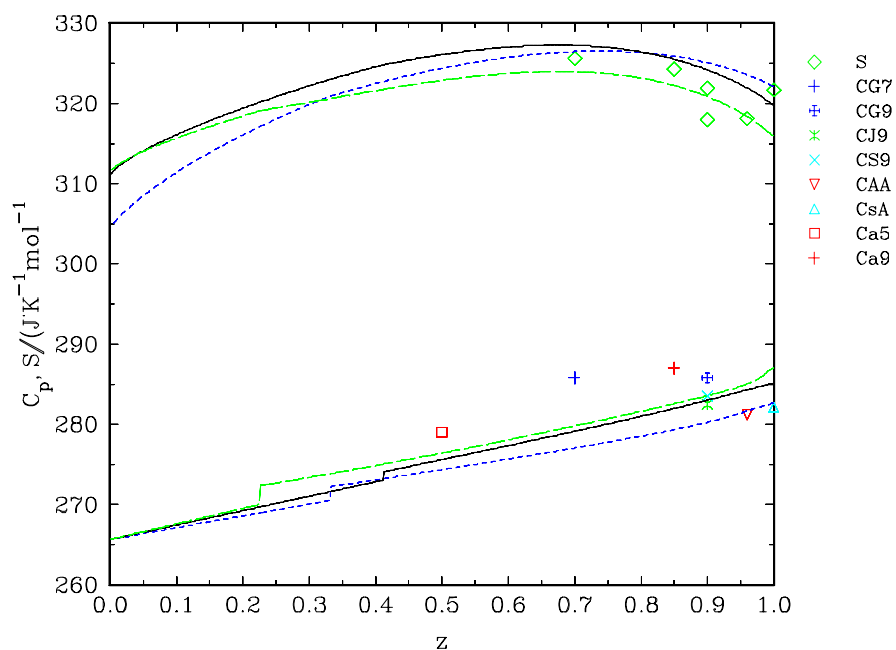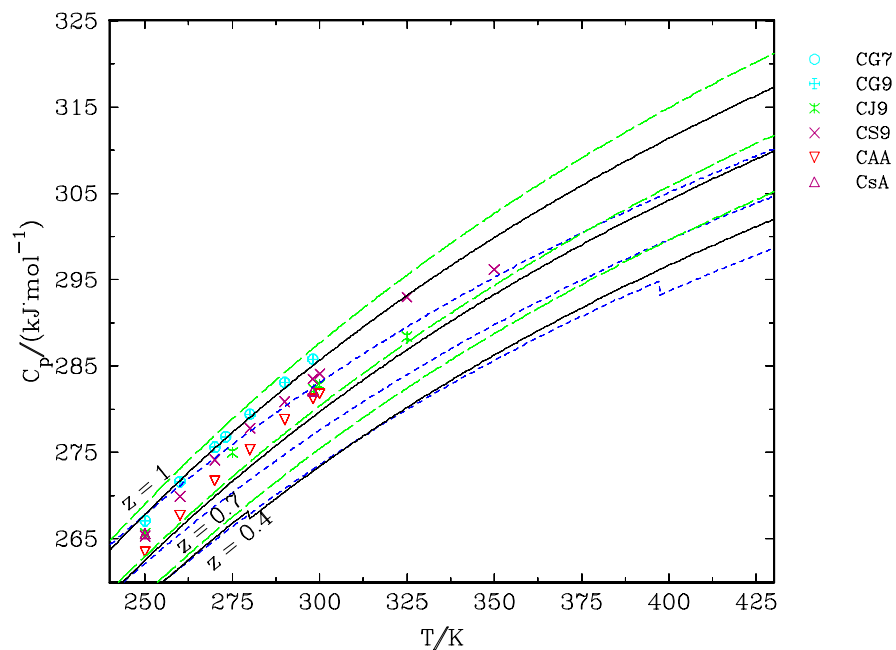**Fig. 3. The order parameter as a function of the temperature at the fixed oxygen partial pressure. The solid line is solution ML, the long dashed line is solution WLS, the short dashed line is the solution by 93DEG/VOR.**
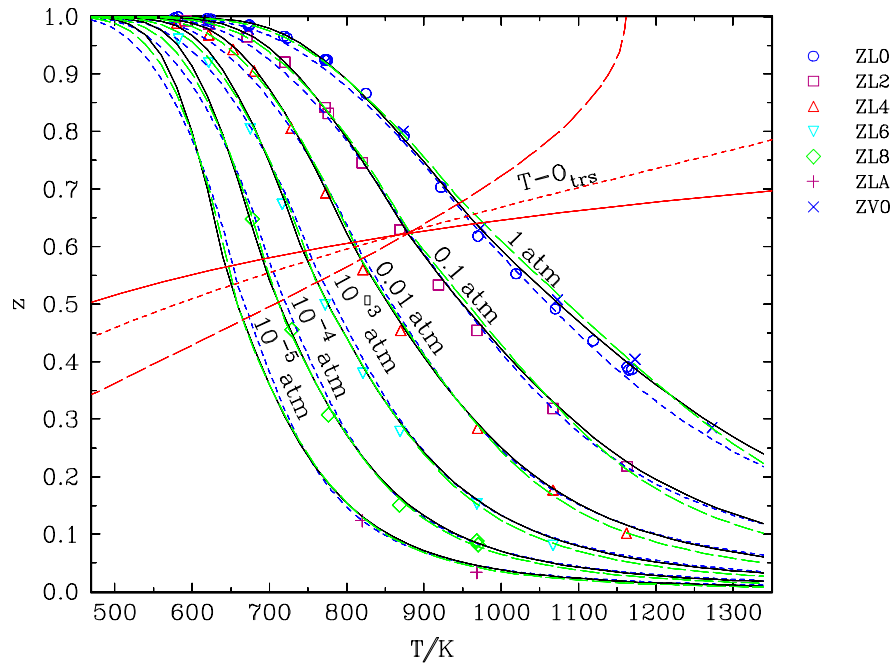
Fig. 4. Index z as a function of the temperature at the fixed oxygen partial pressure: 89LIN/HUN and 89VER/BRU. The solid line is solution ML, the long dashed line is solution WLS, the short dashed line is the solution by 93DEG/VOR.
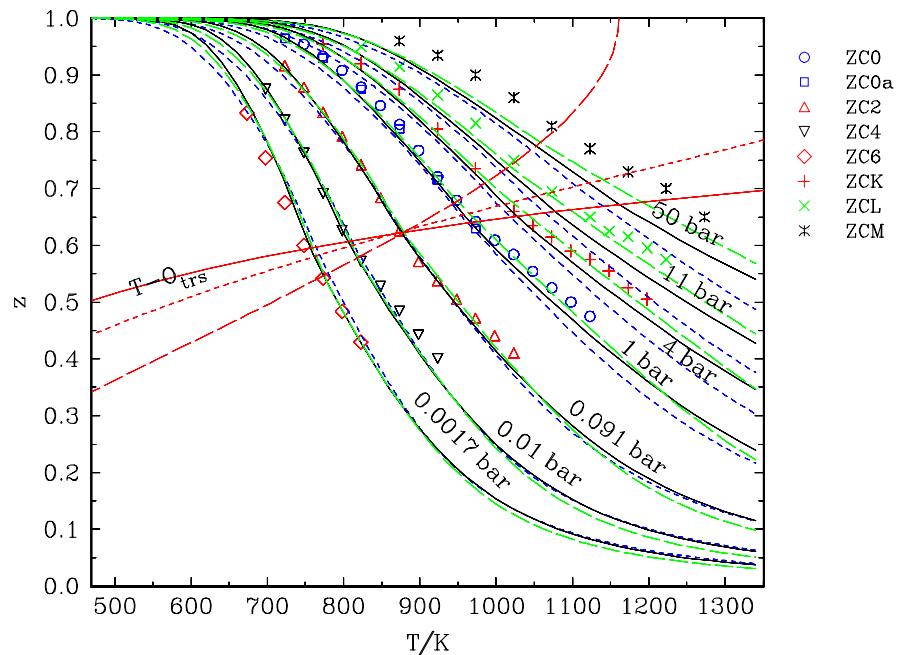
Fig. 5. Index z as a function of the temperature at the fixed oxygen partial pressure: 92CON/KAR. The solid line is solution ML, the long dashed line is solution WLS, the short dashed line is the solution by 93DEG/VOR.

Fig. 6. The oxygen partial pressure as a function of index z at constant temperature: 89GER/PIC and 91SCH/HAR. The solid line is solution ML, the long dashed line is solution WLS, the short dashed line is the solution by 93DEG/VOR.

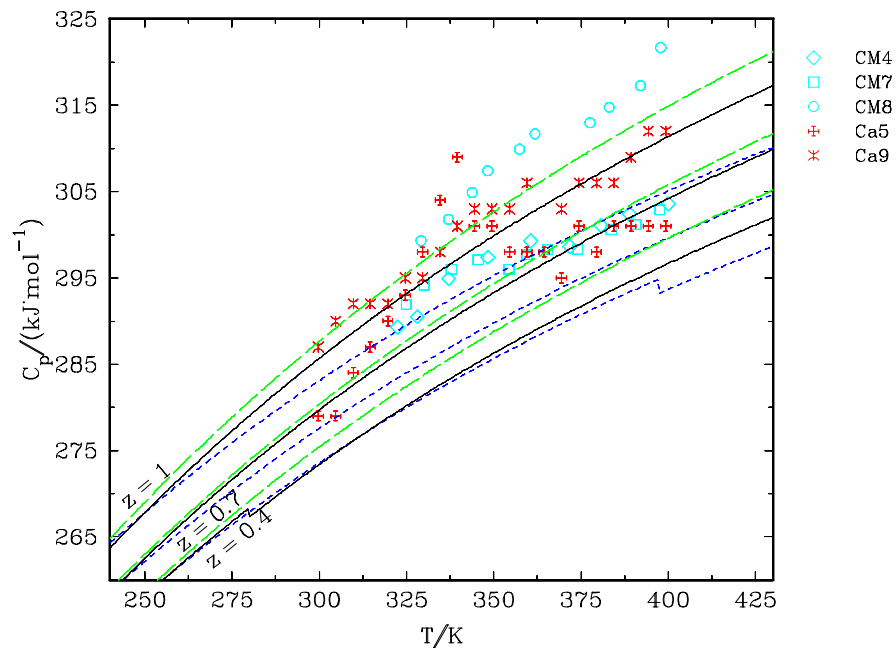**Fig. 7. The oxygen partial pressure as a function of index z at constant temperature: 92MAT/JAC. The solid line is solution ML, the long dashed line is solution WLS, the short dashed line is the solution by 93DEG/VOR.**

Fig. 8. The oxygen partial pressure as a function of the inverse temperature at constant *z*. The solid line is solution ML, the long dashed line is solution WLS, the short dashed line is the solution by 93DEG/VOR.

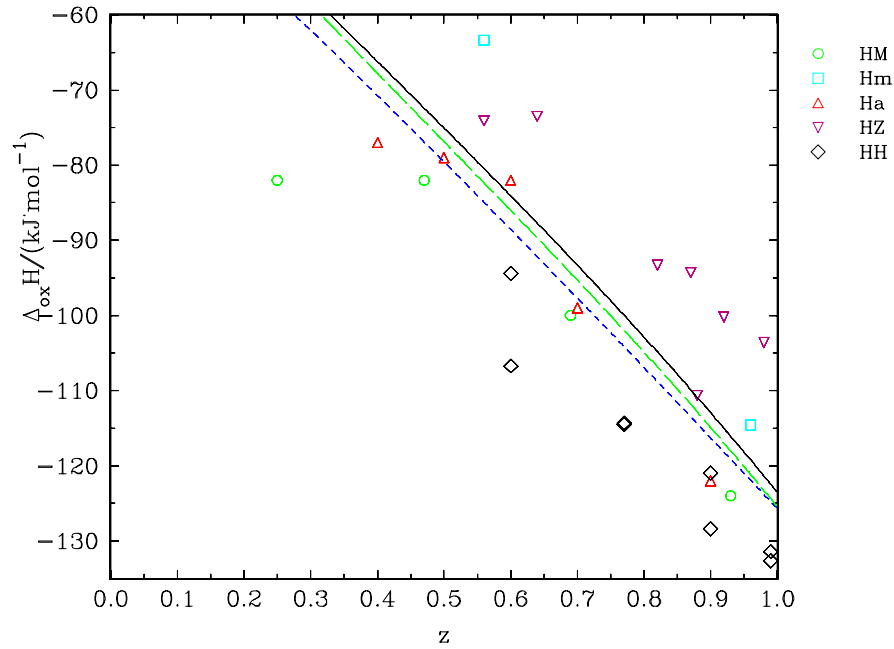**Fig. 9. The partial enthalpy as a function of index z at 873 K (89GER/PIC). The solid line is solution ML, the long dashed line is solution WLS, the short dashed line is the solution by 93DEG/VOR.**

Fig. 10. The enthalpy of Reaction (25) as a function of index z (89PAR/NAV). The solid line is solution ML, the long dashed line is solution WLS, the short dashed line is the solution by 93DEG/VOR.

Fig. 11. The entropy and the heat capacity as functions of index z at 298.15 K. The solid line is solution ML, the long dashed line is solution WLS, the short dashed line is the solution by 93DEG/VOR.
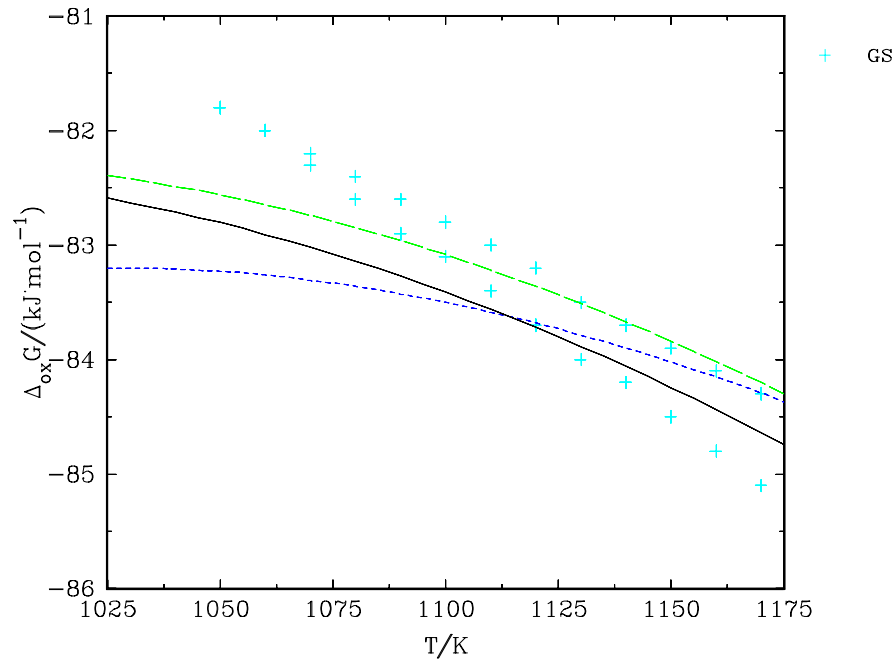
Fig. 12. The heat capacity as a function of the temperature at fixed index z **(adiabatic calorimetry). The solid line is solution ML, the long dashed line is solution WLS, the short dashed line is the solution by 93DEG/VOR.**

Fig. 13. The heat capacity as a function of the temperature at fixed index z **(DSC). The solid line is solution ML, the long dashed line is solution WLS, the short dashed line is the solution by 93DEG/VOR.**

Fig. 14. The enthalpy of formation from oxides as a function of index z at 298.15 K. The solid line is solution ML, the long dashed line is solution WLS, the short dashed line is the solution by 93DEG/VOR.

Fig. 15. The Gibbs energy as a function of the temperature at the fixed oxygen partial pressure equal to 1 atm. The solid line is solution ML, the long dashed line is solution WLS, the short dashed line is the solution by 93DEG/VOR.
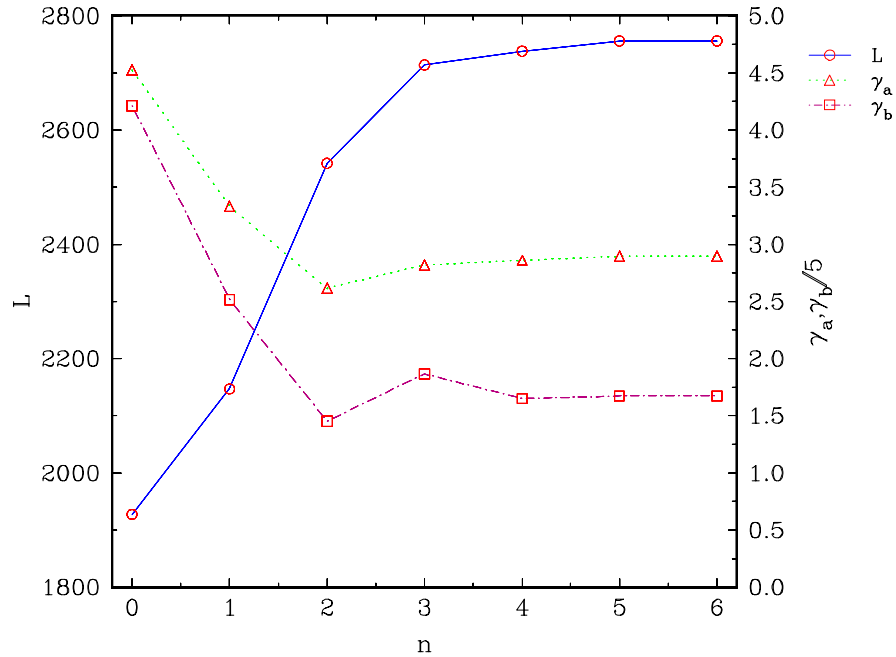
Fig. 16. The dependence of the likelihood function and the ratios, $\gamma_{a,i}$ and $\gamma_{b,i}$ on number of terms in the first sum of Eq. (2).
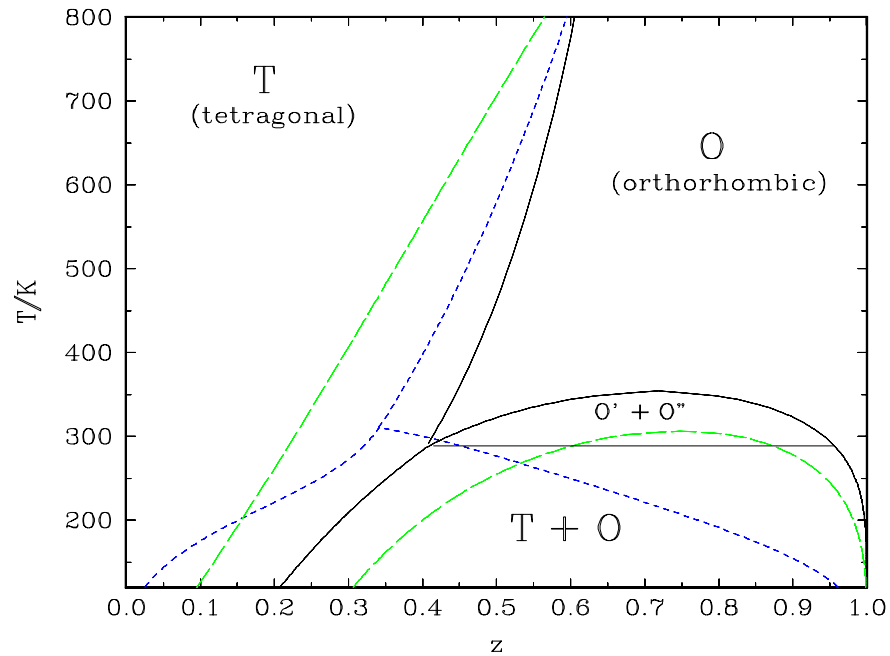
Fig. 17. Phase transformation diagram of the YBa$_2$Cu$_3$O$_{6+z}$ phase. The solid line is solution ML, the long dashed line is solution WLS, the short dashed line is the solution by 93DEG/VOR.
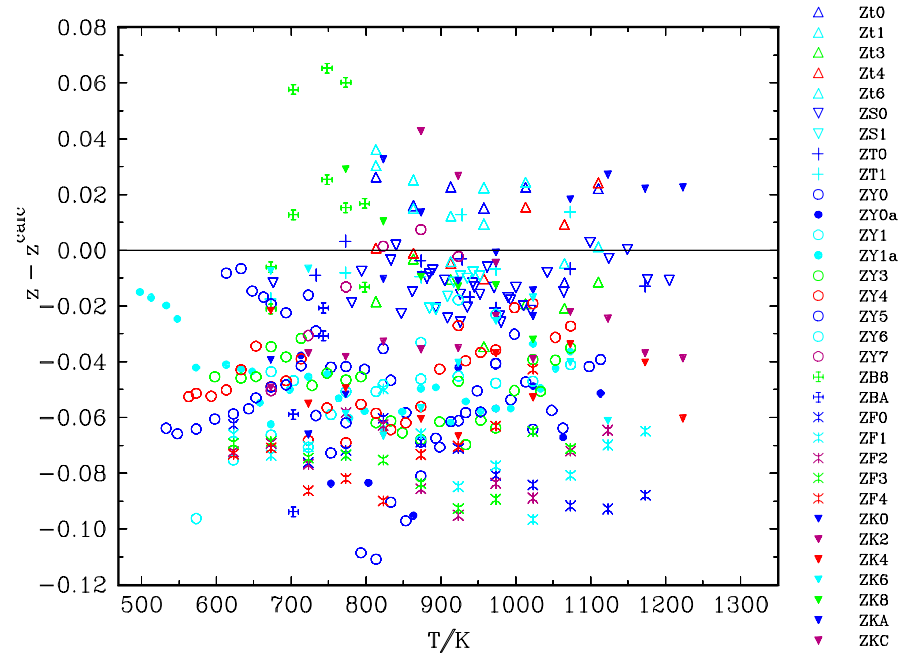
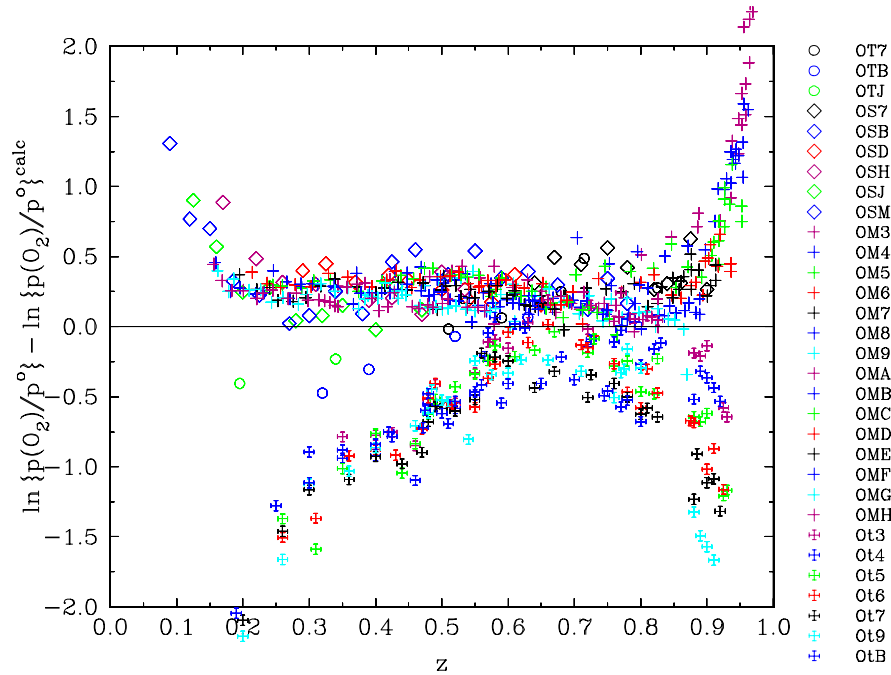**Fig. 18. Deviates for the experiments in group Z_g for solution ML.**

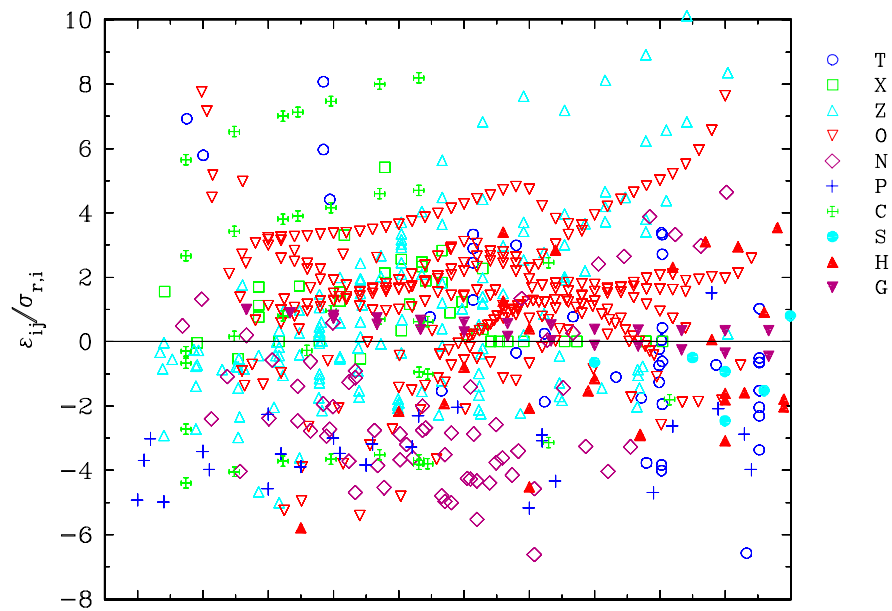**Fig. 19. Deviates for the experiments in group O_g for solution ML.**

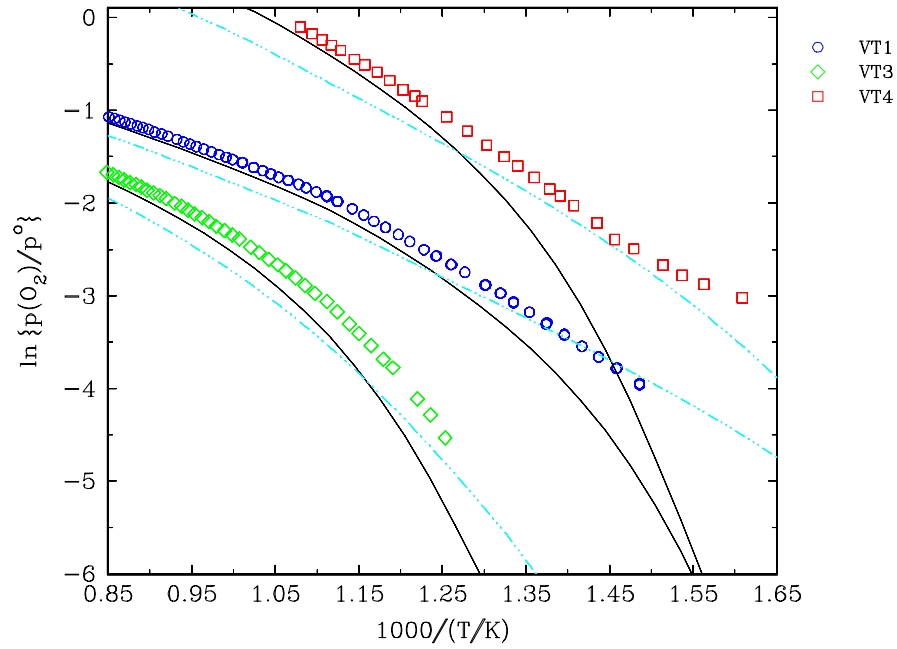**Fig. 20. Normalized deviates for all the experimental points included into the assessment for solution ML.**

Fig. 21. Tilt systematic error versus shift systematic error for solution ML. The code of the experiment is used as a mark.

Fig. 22. Tilt systematic error versus shift systematic error for 93DEG/VOR. The code of the experiment is used as a mark.

Fig. 23. The total pressure as a function of inverse temperature in 94TAR/GUS. The solid line is solution ML, the dot dashed line is solution TAR.

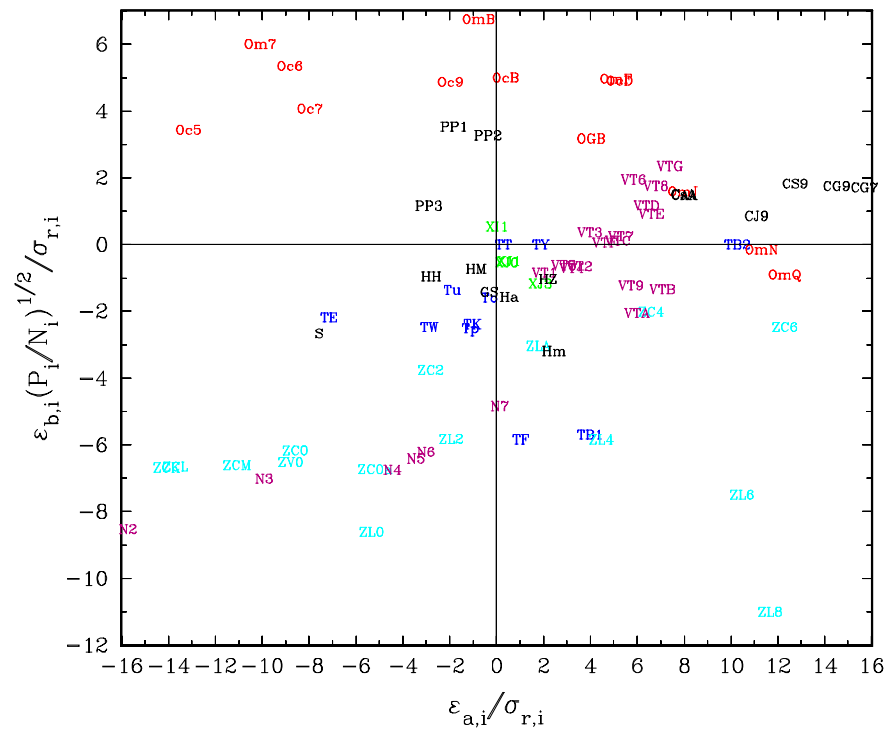
Fig. 24. Tilt systematic error versus shift systematic error for solution TAR. The code of the experiment is used as a mark.
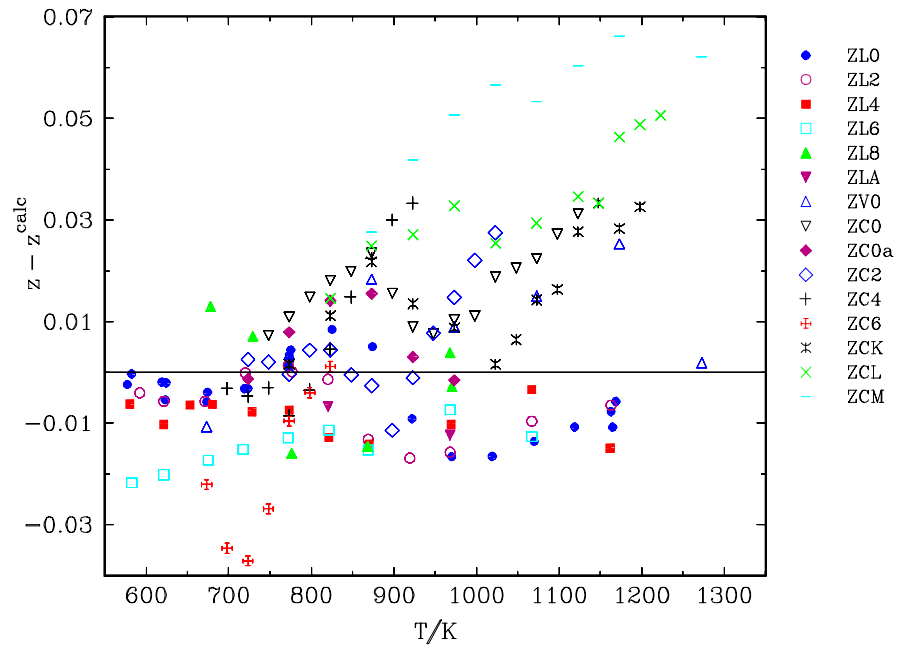
Fig. 25. Tilt systematic error versus shift systematic error for solution WLS. The code of the experiment is used as a mark.

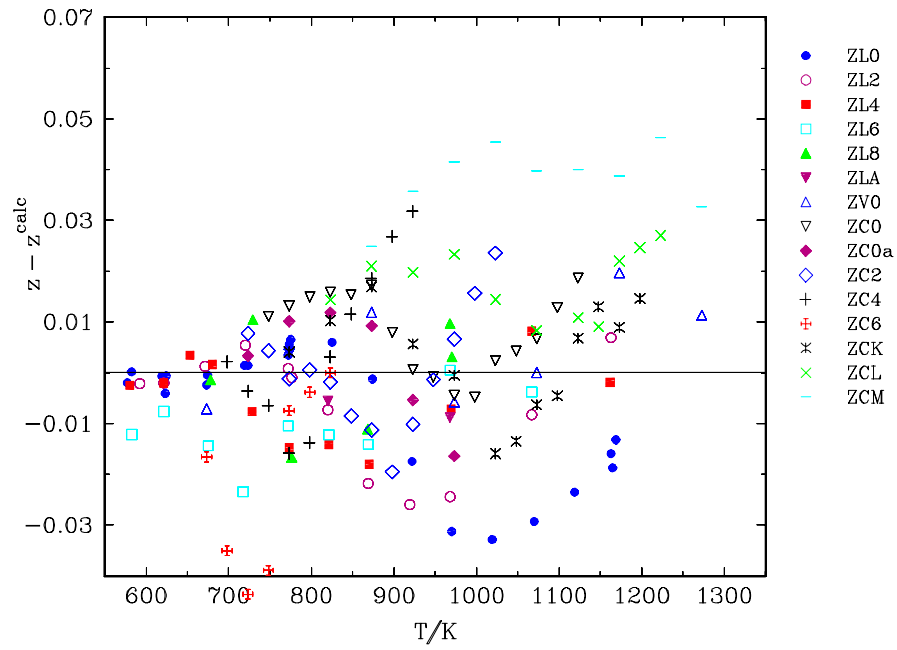**Fig. 26. Deviates for the experiments in group Z for solution ML.**

Fig. 27. Deviates for the experiments in group Z for solution WLS.